LASER NONENHANCEMENT OF BETA DECAY

by

IRA BLEVIS

B.Sc.,University Of Toronto,1981

A THESIS SUBMITTED IN PARTIAL FULFILMENT OF

THE REQUIREMENTS FOR THE DEGREE OF

MASTER OF SCIENCE

in

THE FACULTY OF GRADUATE STUDIES

Department Of Physics

We accept this thesis as conforming

to the required standard

THE UNIVERSITY OF BRITISH COLUMBIA

June 1984

In presenting this thesis in partial fulfilment of the requirements for an advanced degree at the University of British Columbia, I agree that the Library shall make it freely available for reference and study. I further agree that permission for extensive copying of this thesis for scholarly purposes may be granted by the Head of my Department or by his or her representatives. It is understood that copying or publication of this thesis for financial gain shall not be allowed without my written permission.

Department of PHYSICS

The University of British Columbia
2075 Wesbrook Place
Vancouver, Canada
V6T 1W5

Date: June 1984

Abstract

The possibility of influencing nuclear beta decay with high intensity, low frequency electromagnetic radiation (such as from a laser) is examined. The motion of an electron in an e.m. field is found first according to classical mechanics and then according to quantum mechanics. The latter discussion yields the Volkov solution for the electron wave function which is then used in a beta decay calculation patterned after Becker *et al*. In this calculation the Volkov solution is substituted for the electron plane wave factor in the transition amplitude in the Fermi theory of beta decay.

The ratio of total decay rates $R=\frac{W^{\text{with Laser}}}{W^{\text{no Laser}}}$ is numerically evaluated with a computer for the case of ^3H (and some others) where the emphasis is on only allowed nuclear transitions and on phase space considerations. No change in rate to 1% accuracy is found, for the range of the dimensionless field strength intensity parameter $\nu=\frac{ea}{m}\in[.3,7]$, or the photon energy range $\omega\in[2,8]$eV. This range of ν corresponds to the range in laser intensity of $I\in[3\times10^{17},2\times10^{20}]W/cm^2$. The endpoints of the neutrino spectrum are found to be unmodified by the laser (both analytically and numerically). Thus this calculation suggests that the basic beta decay process is not affected by laser irradiation.

Table of Contents

List of Tables

List of Figures

Acknowledgement

Thanks are extended to Dr. D. Beder of the Department of Physics of UBC for both suggesting and supporting this research. My gratitude to Dr Beder, Dr. N. Weiss, and their colleagues for the enrichment of my graduate school program is also due.

I. INTRODUCTION

1.1 History

The possibility of influencing nuclear beta decay processes by intense laser beams recently stimulated some interest following the publication of Becker et al (ref. 2, 1981). The laser modified differential decay rate was presented along with some dramatic numerical results. For low energy allowed decays, namely for ^{3}H and ^{18}F with e^- energies of 18 KeV and 650 KeV, and for laser intensities of about 10^{18} W/cm^2, they claimed enhancements in the decay rate by factors of up to 10^4. Their paper outlined the calculation showing key expressions and important parameters but omitted the details of a difficult integral. Subsequently they published a note (ref. 4, 1983) refuting their original result without commenting on it directly. The first letter used a Fourier Bessel series expansion in the Volkov solution, representing the electron, to arrive at an expression for the differential decay rate. This apparently was integrated analytically, but details of the integration were not included. The subsequent note used the approximate integration technique of steepest descent to arrive at a simple expression for the total decay rate from which the laser parameters cancelled.

Since the first letter others have repeated and augmented the work. John Hebron (ref. 14, 1983) included an explicit calculation of the differential decay rate expression in his M.Sc. thesis. He also included a

discussion of a one dimensional square well nuclear model to argue against the first result of Becker et al. In preparation of the present thesis the differential decay rate calculation has been repeated and the decay rate expression has again been verified. Riess (ref. 19, 1983) has performed similar work; but his emphasis was on forbidden decays and as with Hebron he did not give numerical results. Ternov et al (ref. 20, 1983) have now published numerical results that show there is no significant enhancement.

The present work has yielded numerical results also showing that there is no enhancement in nuclear beta decay. The summation of large order Bessel functions that appears in the differential decay rate, and the integration to find the total decay rate were performed numerically. Although the differential rate was dependent on the intensity of the laser, the total decay rate was insensitive to this and was equal to the unmodified rate. As well the neutrino spectra was found to be unshifted by the laser. These results are to be submitted for publication shortly in collaboration with D.S. Beder.

1.2 First Impressions

Becker et al proposed that the quantum states of the charged particles produced in β decay were modified by the laser flux, increasing the number of accessible states for a decay and consequently , using the Fermi Golden rule (ref. 5) increasing the decay rate. To elucidate this suggestion,

first beta decay and the number of accesible states is considered, then general arguments concerning the possible effects of a laser are presented, in this chapter. A detailed calculation and final results contained in the succeding chapters complete the discussion.

In β decays considered herein, the energy and momentum are shared amongst three particles in the final state. Initial considerations have the particles contained in a large but finite volume in coordinate space (a box) and thus to have discrete energy spectra. One particle, the nucleus, is much more massive than the others and acquires proportionately little of the decay energy as dictated by the law of conservation of momentum. Most of the energy is distributed to the two leptons. The configurations are not constrained except by energy-momentum conservation and all possibilities would be realized in a statistical ensemble of decays. If the energy of the decay were higher, then the number of possible configurations would also be higher as would the total probability of decay for a given time interval.

The counting argument of the last paragraph is suggestive regarding the case of an infinite box and continuous spectra. The phase space domains allowed by energy conservation are Riemann integrable, continous, and constrained by the total energy available for the decay. Larger decay energies entail larger domains in phase space which entail higher decay probabilities, as for the discrete

case. It is a success of β decay theory that the wide variations in decay rates found in nature can be explained by such phase space arguments.

In a semi-classical approach to β decay in a laser field, the energy, Q>Kev, might be thought of as the energy necessary to convert a virtual β decay into a real one: fig 1.

Figure 1 - Virtual and Real β Decay

This energy and the Heisenberg uncertainty principle determine a time interval and thus an energy absorption rate for the virtual e^-

$$Q\,\Delta t \geq \hbar$$

$$\therefore \quad P = \frac{Q}{\Delta t} = \frac{Q^2}{\hbar} \approx 10^{15}\ MeV/s$$

If the virtual e^- responds to the electric force (the Lorentz force is weaker by 1/c) of a laser $\nu = 1$, $\omega = 2eV$, for this Δt, then the absorbed power is

$$P \approx \nu^2 m_t \omega^2/\hbar^2 \approx 10^{10}\ MeV/s$$

Consequently we are not led to an expectation of enhancement of β decay by this route.

In a quantum mechanical approach to β decay in a laser field, the large difference in scale size (wavelength) of

the β decay phenomena (Q>KeV) and the laser field photons ($\omega \approx$ eV) leads initially to no expectations of a significant interaction in analogy to the resonance phenomenon. But the most intense lasers available today can provide ~~intensities~~ of light to atomic sized regions of about 10^{20} times ~~that~~ the intensity of the usual laboratory environment for β decay experiments (about 10^{-2}W/cm^2). Thus even if there is only a small coupling, at this intensity the modification of the rate could possibly be significant. [1]

To calculate the magnitude of this effect the electrically charged particles are coupled to the laser photon field. Then the transition rate for the β decay process is recalculated. As a first approximation the nuclear response to the laser flux may be neglected relative to the β particle's response. This calculation comprises the body of the thesis and is outlined in the next section. In light of the above discussion of β decay rates attention will be given to whether the laser flux increases the number of accessible states. It will be seen that the total decay rate does not change (sec 4.6) and that the neutrino spectrum retains its original bounds (sec 4.2); the latter result is consistent with no increase in rate, and no modification of the β decay process.

---

[1] The assumption that the nucleus of an atom or ion may be exposed to the laser flux has been debated in the literature (ref. 2,3,13,14) as has the possibility of experimentaly distinguishing β particles from background (ref. 2,3,14,18) Only the question of the theoretical existence of an effect will be considered in this work.

1.3 Outline

Chapter 2 is a discussion of the motion of an electron, (or charged particle), under the influence of the e.m. field of a laser. The classical solution included is useful for building intuition and the quantum solution for the β decay calculation that follows.

Then the quantum calculation of the decay rate is presented; chapter 3. It begins with general considerations in order to shed some light on the basic physics. These considerations involve some phenomenology governing the Hamiltonian, but then the discussion centers on unpolarized nuclear transitions, unobserved final polarizations of leptons, and unobserved neutrino momenta. These quantities are summed or integrated out of the decay rate expression early in the discussion economizing on labour. Induced decay is then treated in a similar manner.

Chapter 4 begins with the determination of the kinematical domains for the differential decay rate and continues with some detail of the numerical work.

Chapter 5 is a conclusion.

1.4 Conventions

Throughout this paper the fundamental unit has been chosen to be energy, MeV. Then other units are derived using $\hbar=1=c$. Electromagnetic units are Gaussian with this modification. For example the charge of the electron is $e=1/\sqrt{137}$, (dimensionless).

The standard summation convention including the use of the metric to map tensors into their dual spaces (raise and lower indices) and the distinction between Latin and Greek indices is also followed; however, vector or tensor notation without indices is also commonly used. Brackets will often enclose a typical term of the tensor they denote, for example $(M^{\alpha\beta})^{\mu\nu}=M^{\mu\nu}$. The duals of geometrical objects will be denoted by a star in componentless notation. For example a 2-tensor has a dual F*=GFG, where G is the metric. The natural inner product for tensors of rank 2 and lower is (X,Y)=tr(XY*). The 'square' shall refer to the inner product of a tensor with itself.

Feynman representation for γ algebra is chosen so that Dirac equation results resemble those of Bjorken and Drell.[2] More detail is displayed in appendix A.

Throughout the thesis m will be the electron mass; other masses will be subscripted. ω will be the laser frequency (energy); other energies will be subscripted. The dimensionless parameter governing the whole effect is $\nu=\frac{ea}{m}$ where e is the electron charge, and a is the field strength of the vector potential representing the laser.

---

[2] Bjorken and Drell, ref 5, appendix A

II. MOTION OF AN ELECTRON IN AN E.M. FIELD

2.1 Classical Solution

Governing equation

The Lagrangians $L_m = \int \frac{m}{\gamma} \delta^4(x-y)\, d^3y$ or $L_m = m\int v^2 \delta^4(x-y)\, d^3y$, defined up to multiplicative constants, lead via a minimizing principle of the action $S = \int L\, dt$ to the Euler-Lagrange equations and to the expected result for a free uncharged particle at x, namly $\vec{a}=0$.

The Lagrangian density $\mathcal{L}_f = -\frac{1}{4} tr\, FF^* = -\frac{1}{4} F_{\mu\nu} F^{\mu\nu}$, formed from the square of the e.m. field tensor, leads in a similar manner to the governing equations of the e.m. fields in vacuum, Maxwell's equations. The $\vec{E}$ and $\vec{B}$ fields can be replaced by potential fields A, (where $F_{\mu\nu} = A_{\mu,\nu} - A_{\nu,\mu}$), a Lorentz 4 vector. The governing equations are now second order in the time derivative, and the dynamical variables resemble those of particle mechanics. The source free Maxwell equations $\partial_\mu F^{\mu\nu} = 0$ are automatically satisfied. The dynamics are given by the wave equation if the Lorentz gauge is chosen.

The Lagrangian density $\mathcal{L} = \mathcal{L}_f + \mathcal{L}_m - J_\mu A^\mu$ including source fields $J = m\int v\, \delta^4(x-y)\, d\tau$, where $v = \gamma(1, \vec{V})$ is the 4-velocity, leads to Maxwell's equations with sources and also accounts for the interaction of the sources with their own fields. Gauge invariance of the Lagrangian is guaranteed by the vanishing divergence of J and the insensitivity of the minimizing procedure to additions of a total derivative to $\mathcal{L}$. Here, as a good approximation the A^μ are assumed to

describe only the laser and the J^μ to describe the mechanical electric current of the point source, the electron.

The Euler Lagrange equations lead to homogeneous wave equations for each of the laser e.m. fields. If k is the lightlike propagation vector for the laser e.m. field and ε is the spacelike polarization, then

$$k^2 = k\cdot\varepsilon = 0 \quad , \quad \varepsilon^2 = -1$$

and solutions of the wave equations are functions, f , of $\varsigma = k\cdot x$

$$A^\mu = \varepsilon^\mu f(\varsigma)$$

The ordinary derivative of a function with respect to its argument will be denoted by " ' ". The piece of the action involving the electron is

$$S = -\int \left(\frac{m}{\gamma} + e A\cdot v\right) dt$$

Though written using the quantities measured in an inertial reference frame, the Euler Lagrange equations

$$\frac{d}{dt}\left(m v + e A\right) - e A'\cdot v \; k = 0$$

can be rearranged to give the familiar covariant Lorentz force equation

$$m \frac{du^\nu}{d\tau} = e \; F^{\nu\mu} \, U_\mu \qquad \text{II.1}$$

where U is the relativistic 4-velocity as stated above.

Solution

The general solution for the motion of this classical particle has been found from the Lorentz equation II.1 by Itzykson and Zuber (ref. 15). Landau and Lifshitz (ref.

17) have also found the solution; they solve the relativistic Hamilton Jacobi equation for Hamilton's principle function and then the dynamic variables, momentum and energy. The approach taken here builds intuition by first solving the Lorentz equation for the simple initial conditions of a particle at rest at the origin. Then the action is calculated to corroberate the literature and to facilitate comparisons with the quantum mechanical solution of the next section. In that case one expects $\psi = e^{iS}$, where S is the action of a trajectory in phase space, to be the probability amplitude that that trajectory is realized by a quantum mechanical particle. Next the lab frame motion is described and then Lorentz transformations are used to show the effects of differing initial conditions. Finally the energy of the particle is related to physical parameters of the laser.

Choosing the z axis of the lab frame as the direction of propagation of the e.m. field is realized by setting $k=(\omega,0,0,\omega)$. For the purpose of illustration f can be chosen as the plane wave $f = a \sin S$ and ε^μ for linear polarization as $\varepsilon^\mu=(0,1,0,0)$. Therefore the laser fields have the usual characteristics

$$FF = 0 \longrightarrow |\vec{E}| = |\vec{B}|$$
$$F^* F^* = 0 \longrightarrow \vec{E} \cdot \vec{B} = 0$$
$$F^{\mu\nu} k_\mu = 0 \longrightarrow \vec{E} \cdot \vec{k} = \vec{B} \cdot \vec{k} = 0$$

We choose the lab frame initial conditions $\vec{x}(0)=\vec{v}(0)=0$,

then $U(0)=(1,\vec{0})$. The Lorentz equation II.1 becomes

$$a)\ \frac{dU^0}{d\tau} = \omega\nu\cos\zeta\, U_1 \qquad c)\ \frac{dU^2}{d\tau} = 0$$

$$b)\ \frac{dU^1}{d\tau} = \omega\nu\cos\zeta\,(U_0+U_3) \qquad d)\ \frac{dU^3}{d\tau} = \omega\nu\cos\zeta\, U_1$$

II.2

where $\nu = \frac{ea}{m}$ is a parameter giving the strength of the interaction relative to the mass of the electron. Comparison of II.2a) and d) gives $\dot{U}^0 = \dot{U}^3$ ie. $U^0 - U^3 = C$, a constant, which equals 1 from initial conditions. Substituting this and $U_0 + U_3 = U^0 - U^3$ into II.2b allows it to integrated. With U^1 now, equations a) and d) can be integrated. Using the initial conditions II.2 becomes

$$a)\ U^0 = \frac{\nu^2}{2}\sin^2\omega\tau + 1$$

$$b)\ U^1 = -\nu\sin\omega\tau$$

$$c)\ U^2 = 0$$

$$d)\ U^3 = \frac{\nu^2}{2}\sin^2\omega\tau$$

The 4-momentum is

$$e)\ P = mU = m\gamma V$$

II.3

Inspection of shows that it can be written as

$$U = U(\infty) - \frac{e}{m}A + C$$

where $U(\infty)$ is a constant depending on initial conditions, $\frac{e}{m}A$ is a component parallel to A, and $C = \frac{e^2}{2m}A^2\frac{k}{k\cdot U}$ is an oscillatory part perpendicular to A. This decomposition is

unique since the initial conditions of the particle, and the directions of polarization and propagation of the laser flux, are all fixed input parameters. Thus the action

$$\begin{aligned} S &= -\int L\, dt \\ &= -\int (m U^2 + 2eA\cdot U)\, dt \\ &= -m\, U(\infty)\cdot x + \int \frac{dS}{n\cdot U}\left(eA\cdot U + \frac{e^2}{2m^2}A^2\right) \end{aligned}$$

II.4

This is a useful expression to compare to the quantum mechanical solution to come.

To better visualize the motion, P_{RMS} that is, in the laboratory frame, we must integrate P from II.3e over the lab frame time t. II.3 can be used to solve for τ in terms of t. To wit:

$$\frac{dt}{d\tau} = \gamma = U^0$$

$$\therefore\ t = \frac{4+\nu^2}{4}\tau - \frac{\nu^2}{8\omega}\sin 2\omega\tau$$

II.5

By inspection we see that $t = \frac{4+\nu^2}{4}\tau$ is an asymptote of II.5 and in fact that the two intersect twice per period with period π/ω for τ, or period $\frac{4+\nu^2}{4}\frac{\pi}{\omega}$ for t. Thus τ is well approximated by

$$\tau = \frac{4}{4+\nu^2}\left(t + \frac{\nu^2}{8\omega}\sin\frac{8\omega}{4+\nu^2}t\right)$$

Figure 2 depicts this.

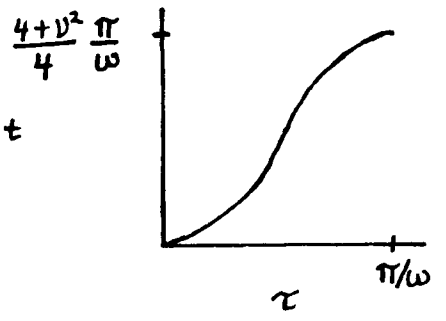

Figure 2 - LAB TIME AND PROPER TIME

We then notice that momentum from II.3 has half the frequency of the figure and thus integrations over integral numbers of periods w.r.t. τ or t are equivalent for finding the P_{RMS} .

$$P_{RMS} = m \begin{pmatrix} (1 + \frac{\nu^2}{2} + \frac{3\nu^4}{32})^{1/2} \\ \nu/\sqrt{2} \\ 0 \\ \frac{\nu^2}{4}\sqrt{3/2} \end{pmatrix} \qquad \text{II.6}$$

One can check that $P_{RMS}^2 = m^2$.

In any frame other than that in which the particle starts at rest we have

$$p_z' = \gamma'(p_z - \beta' p_0)$$

$$p_z' = m\gamma' \left(-\beta' - \frac{\nu^2}{4}\beta'(1-\cos 2\omega\tau)\right) \qquad \text{II.7}$$

where $\gamma' = (1 - \beta'^2)^{-1/2}$, and $\beta' = \vec{v}(0)$, the initial velocity of the electron. Thus in any frame the motion of the electron is a constant plus oscillating terms. Though we have not included reradiation effects, the electron achieves a quasistationary momentum state. This is attributable to the oscillatory nature of the Lorentz force in the z direction, or one may regard the onset of the e.m. field as contributing a net impulse to the electron in the z direction. Our approximation of not including electron field effects is vindicated by comparing the magnitudes of the radiation damping force to the acting external force. The radiation damping force from energy conservation considerations[3] in the lab coordinates is

$$F_{rad} = \frac{2}{3} e^2 \ddot{v}$$

The acting force is the Lorentz force

$$F_L = m\dot{v}$$

The ratio of the two is of order $\frac{e^2\omega}{m}$ which in our units is about $2 \times 10^{-6}/137$ or 10^{-8}.

To relate these calculations to real consequences we must relate the experimental laser power to the parameters here. To ensure confidence, the Poynting vector that has been used with great experimental success[4] to represent the energy flux of the e.m. fields is rederived in the following combination of natural and Gaussian units. We

---

[3] Jackson, ref. 16, p784

[4] See Feynman Lectures, ref. 11, II 27-4 "Ambiguities of the Field Energy".

have already used $\hbar=1=c$ to reflect the freedom of choice of units. Including sources in Maxwell's equations, and choosing the Coulomb's law and Ampere's law constants appropiately gives the Maxwell's equations in the form

$$a) \quad \vec{\nabla}\cdot\vec{E} = 4\pi\rho$$

$$b) \quad \vec{\nabla}\times\vec{B} - \frac{d\vec{E}}{dt} = 4\pi\vec{J} \qquad \text{II.8}$$

The rate that work is done on a charge e when it responds to a field $\vec{E}$ with a velocity $\vec{v}$ is $P=\vec{E}\cdot e\vec{v}=\vec{E}\cdot\vec{J}$. Conventionally $\vec{J}$ is replaced from II.8b

$$P = \vec{E}\cdot\vec{J} = \frac{1}{4\pi}\left(\vec{E}\cdot\vec{\nabla}\times\vec{B} - \vec{E}\cdot\frac{d\vec{E}}{dt}\right)$$

$$= \frac{1}{4\pi}\left(\vec{\nabla}\cdot\vec{E}\times\vec{B} + \vec{B}\cdot(\vec{\nabla}\times\vec{E}) - \frac{1}{2}\frac{dE^2}{dt}\right)$$

$$\therefore \quad P = \frac{1}{4\pi}\vec{\nabla}\cdot(\vec{E}\times\vec{B}) - \frac{1}{2}\left(\frac{d(E^2+B^2)}{dt}\right)$$

Then $\frac{d}{dt}\frac{E^2+B^2}{8\pi}$ is identified as the rate of loss of energy from the e.m. field and $\nabla\cdot(\vec{E}\times\vec{B})/4\pi$ as the flow of energy out of a point. If $\vec{J}=0$ then one says that $\vec{S}=\vec{E}\times\vec{B}/4\pi$ is the energy flux of the e.m. field. As mentioned earlier the truth of this assertion is its experimental success, but our purposes have been served as we now have Poynting's vector, $\vec{S}$, in our units. Time averaging the magnitude of $\vec{S}$ using the previous definitions of the field tensor gives

$$I = \langle|\vec{S}|\rangle = a^2\omega^2/8\pi$$

For a laser of $I=10^{18}W/cm^2$, and $\omega=2eV$, we have

$$a^2 = 3.922 \times 10^{17} / MeV\text{-}s\text{-}f^2$$

Thus

$$\nu^2 = \frac{e^2a^2}{m^2} = .281$$

and

$$\nu = .530$$

From II.6

$$E_{RMS} = 1.07\, m$$

and for $\nu = 1$

$$E_{RMS} = 1.26\, m \qquad \text{II.9}$$

Recall that the mass of the electron is measured in natural units, Mev.

2.2 Volkov Solution

Governing Equation

The original conception was to use the wave function of an electron in a plane electromagnetic field in the beta decay transition amplitude. This wave function is the Volkov solution (ref. 21, 1935) to the Dirac equation with a minimal coupling interaction. It is now rederived and then compared to the classical solution to see that it is reasonable.

The Hamiltonians of classical mechanics involve canonical, or standard, variables which are replaced by canonical operators in the succesion to quantum mechanics. Ordinary quantum mechanics uses these operator Hamiltonians as the generators of time translations (Schrodinger's equation). Incorporating special relativity (by finding Lorentz covariant equations) into quantum mechanics was accomplished by using relativistic Hamiltonians. Originally proposed to overcome problems of interpretation related to

the Klein-Gordon Hamiltonian or its square root, the Dirac Hamiltonian was found to imply the fermion spin-statistics connection (ref. 5).

To describe a charged particle in an external electromagnetic field, classical correspondence can be invoked to justify the use of the conjugate momentum p-eA in place of p in the first order equation, the Dirac equation. The same result can be found from the canonical quantization procedure utilizing a Lagrangian. The Lagrangian is formed from a term calculated to lead to the Dirac equation for the electron, a term to describe the electromagnetic field, and an interaction term. As in the classical case the charged particle's own field may be neglected. The Lagrangian density is

$$\mathcal{L} = \bar{\Psi}(x)\,(\hat{\not{p}} - m)\,\Psi(x) - \tfrac{1}{4} F^2(x) - e\,\bar{\Psi}(x)\,\not{A}(x)\,\Psi(x)$$

and the Euler Lagrange equations of motion involving the particle are

$$\hat{\mathcal{D}} \equiv (\hat{\not{p}} - e\,\not{A} - m)\,\Psi(x) = 0 \qquad \text{II.10}$$

($\hat{\not{p}} \equiv \gamma^\mu \hat{p}_\mu$, $\hat{}$ denotes operators, and $\hat{1}$ is implicit) Further justification (if it is needed) for this governing equation is that it is required by the necessity of invariance of the Dirac equation under local gauge transformations. These transformations involve the addition of the gradient of a function $\partial_\mu \Theta(x)$ to the vector potential and the simulataneous multiplication of the wave function by a phase factor $e^{ie\Theta(x)}$ whose argument is that gauge function. $\hat{\not{p}}$ -eA

is the covariant derivative for this group of transformations.

Solution

After the models of Landau and Lifshitz and Itzykson and Zuber we solve for Ψ by first looking for a second order equation. To this end we multiply by $\hat{p}-e\not{A}+m$ and find

$$[(i\partial_\mu \gamma^\mu - e A_\mu \gamma^\mu)^2 - m^2]\Psi = 0$$

$$\therefore \quad [\gamma^\mu \gamma^\nu (i\partial_\mu - eA_\mu)(i\partial_\nu - eA_\nu) - m^2]$$

$\gamma^\mu\gamma^\nu$ has a symetric part $G^{\mu\nu}$ and an antisymetric part $\sigma^{\mu\nu}$ (eq. A.6). $\sigma^{\mu\nu}$ projects to the antisymmetric subspace of its range. That antisymmetric part of the above operator is

$$\frac{1}{2}[i(\partial_\mu - eA_\mu)(i\partial_\nu - eA_\nu) - (i\partial_\nu - A_\nu)(i\partial_\mu - eA_\mu)]$$
$$= \ldots$$
$$= \frac{1}{2} ie F_{\mu\nu}$$

and is an additional term to that which results from the minimal substitution into the Klein-Gordon equation. It represents a spin interaction with the e.m. field. Thus we have

$$[(i\partial - eA)^2 - \frac{1}{2} e \sigma^{\mu\nu} F_{\mu\nu} - m^2]\Psi = 0 \qquad \text{II.11}$$

Now, as in the analysis of the classical case, we choose an electromagnetic plane polarized plane wave

$$A_\mu = \varepsilon_\mu f(k\cdot x)$$

where

$$k^2 = k\cdot\varepsilon = 0 \ , \quad \varepsilon^2 = -1$$

The spin term becomes

$$\frac{1}{2}\, e\, \sigma^{\mu\nu} F_{\mu\nu} = e\, \sigma^{\mu\nu} k_\mu A'_\nu$$

Using A.6 and 7 this can be rearranged to

$$\frac{1}{2}\, e\, \sigma^{\mu\nu} F_{\mu\nu} = ie(\not{k} \not{A}' - k\cdot A')$$

and since

$$k\cdot A' = k_\mu \varepsilon^\mu f'(k\cdot x)$$

this is

$$\frac{1}{2}\, e\, \sigma^{\mu\nu} F_{\mu\nu} = ie \not{k} \not{A}'$$

The momentum term $(i\partial - eA)^2$ becomes

$$(i\partial - eA)^2 = \ldots = -\Box - 2ieA\cdot\partial + e^2 A^2$$

since we can choose the gauge $\partial_\mu A^\mu = 0$ (Lorentz gauge). The Dirac equation II.11 has now been transformed into

$$[\, -\Box - 2ieA\cdot\partial + e^2A^2 - m^2 - ie \not{k} \not{A}' \,]\, \psi = 0$$

II.12

and we can look for plane wave solutions of the form

$$\psi(x) = e^{i p\cdot x}\, \varphi(k\cdot x)$$

II.13

Since the $\xi = k\cdot x$ dependence is contained in φ, which is yet to be determined, we are free to extract factors of $e^{i\lambda k\cdot x}$ from φ. Thus we may use a redefined constant vector $p = p + \lambda k$ that lies on the mass shell: $p^2 = m^2$.

in II.13 Upon substitution of II.13 into II.12 we find the first term is

$$\left(\begin{array}{l} \partial_\mu \psi = -i p_\mu \psi + e^{ip\cdot x} \varphi'(\xi)\, k_\mu \\ \partial_\mu \partial^\mu \psi = -i p_\mu (-i p^\mu \psi + e^{ip\cdot x} \varphi'(\xi)\, k^\mu) \\ \qquad\qquad -i p^\mu e^{ip\cdot x} \varphi'(\xi)\, k_\mu + e^{ip\cdot x} \varphi'' k^2 \\ \qquad k^2 = 0 \end{array} \right)$$

$$\Box \psi = p^2 \psi - 2 i p\cdot k\, e^{ip\cdot x} \varphi'(\xi)$$

II.14

The second term is

$$2ieA\cdot\partial\psi = 2ieA^\mu(-i p_\mu \psi + e^{-ip\cdot x} \varphi'(\xi) k_\mu)$$
$$= 2eA\cdot p\, \psi$$

II.15

Thus II.12 becomes

$$(p^2-m^2)\psi - 2eA\cdot p\psi + e^2A^2\psi - ie\, k\!\!\!/ A'\psi + 2ip\cdot k\, e^{-ip\cdot x}\varphi'(\xi) = 0$$

II.16

Using $p^2=m^2$ and dividing out the phase yields

$$[-2eA\cdot p + e^2A^2 - ie\, k\!\!\!/ A'\,]\,\varphi(\xi) + 2ip\cdot k\,\varphi'(\xi) = 0$$

II.17

This can be integrated to give

$$\varphi(\xi) = \varphi_0 \exp\left[\int \frac{e^2A^2 - 2eA\cdot p - ie\not{k}\not{A}'}{-2ip\cdot k}\, d\xi'\right] U$$

$$= \varphi_0 \exp\left[\int \frac{e^2A^2 - 2eA\cdot p}{2p\cdot k}\, d\xi'\right] e^{\frac{\not{k}\not{A}}{2p\cdot k}} U$$

II.18

where φ_0 is an integration constant. U is a Dirac spinor as can be seen by substituting it back into the governing equation.

First, eq. A.2 gives that $(\not{k}\not{A})^r = 0$ for $r \geq 1$ and we can rewrite the second exponential of φ as

$$e^{\frac{e\not{k}\not{A}}{2p\cdot k}} = 1 + \frac{e\not{k}\not{A}}{2p\cdot k}$$

Thus the Volkov solution is

$$\psi_{VOL} = \varphi_0\, e^{iS}\left(1 + \frac{e\not{k}\not{A}}{2p\cdot k}\right) U$$

$$S \equiv -p\cdot x + \int \frac{e^2A^2 - 2eA\cdot p}{2p\cdot k}\, d\xi'$$

II.19

where S has been so named because it is the classical action (see section 1.1). The factor in brackets and U results from the spin interaction term. The rest would have resulted from the use of the Klein-Gordon equation from the outset. Normalization, $\varphi_0 = 1$, is found by letting $a \to 0$ lead to the plane wave solution. The factor e^{iS} has the effect of giving the most constructive probability amplitude superpositions to those trajectories for which $\delta S = 0$. That is, the classical trajectory is the most likely one, as expected.

Checking now for the conditions on U we have

$$\hat{\mathcal{D}}\psi = \left(\not{p} - \frac{e}{2ip\cdot k}\left(eA^2 - 2A\cdot p - ie\not{k}\not{A}\right) i\not{k} - e\not{A} - m\right)\cdot \left(1 + \frac{e\not{k}\not{A}}{2p\cdot k}\right) e^{iS} U$$

Dropping terms with $\not{k}\not{k}=0$ and using A.1,2,3 to commute $1+\frac{e\not{n}\not{A}}{2p\cdot n}$ to the left allows the continuation

$$\hat{\mathcal{D}}\psi = \left[\left(1+\frac{e\not{k}\not{A}}{2p\cdot k}\right)\left(\not{p}-m-eA\right) - \left(eA^2 - 2A\cdot p\right)\frac{e\not{k}}{2p\cdot k} + \frac{e2k\cdot p\not{A}}{2p\cdot k} - \frac{e2kA\cdot p}{2p\cdot k}\right] e^{iS} U$$

which reduces to

$$\hat{\mathcal{D}}\psi = \left(1+\frac{e\not{k}\not{A}}{2p\cdot k}\right)\left(\not{p}-m\right) e^{iS} U$$

II.20

Thus $\hat{\mathcal{D}}\psi = 0$ implies that $(\not{p}-m)U = 0$, i.e. that U is a Dirac momentum eigenspinor. It is normalized the same way (ref. 5). These results are corroborated by letting $A \to 0$. The Dirac equation is recovered; plane wave solutions are recovered; and normalized Dirac momentum eigenspinors are also recovered.

Thus the Dirac equation including electromagnetic interactions has been solved in closed form. Usually the state of a system of unperturbed Hamiltonians evolves in Hilbert space covering a parameterized trajectory when interactions are included in the Hamiltonian. Our solution

which looks asymptotically[5] like a momentum eigenstate is such a trajectory Writing our Dirac equation as $(i\partial_0 - \mathcal{H})\psi = 0$ shows that we have not found the stationary states (eigenstates) of : we readily see that ψ_{vol} are eigenstates of $\hat{p}_1$, $\hat{p}_2$ and $\hat{p}_0 + \hat{p}_3$ with eigenvalues p_1, p_2 and $p_0 + p_3$ respectively. Each trajectory $\psi_{p,s}(x) = \psi_{vol}$ has a characteristic x and y momentum and for each the difference of energy and z-momentum is a constant. However energy and z momentum do vary around average values, as seen for the classical motion.

To compare with the calculations of Becker et al a circularly polarized laser e.m. field is used. This is a linear combination of plane polarized plane wave solutions to the wave equations, that differ in their phase by a constant $\pi/2$. We have

$$(A^\mu) = a\,(0, \cos\varsigma, \sigma\sin\varsigma, 0)\,, \quad \sigma = \pm 1$$

$$A\cdot p = a(p_1\cos\varsigma + \sigma p_2 \sin\varsigma)$$

$$\equiv a\,p_\perp \cos(\varsigma - \sigma\psi)$$

$$A^2 = -a^2$$

II.21

where ψ is the azimuthal angle of $\vec{p}$. Thus

$$S = -\tilde{p}\cdot x + \frac{ae}{p\cdot k}\,p_\perp \sin(\varsigma - \sigma\psi)$$

---

[5] The difference of the functions decreases faster than any power function as we look to infinity for the argument.

where $\tilde{p}=p+\frac{e^2a^2}{2p\cdot k}k$. $p_\perp$ is the component of momentum perpendicular to k (and to $\vec{k}$); $p\cdot k=p_\parallel\omega$ is the parallel component. It can be seen that ψ_{VOL} involves e^{iS}, that is, sinusoidal variations modified by trigonometric functions in the frequency. This is reminiscent of Bessel functions. In fact $e^{iz\sin(\zeta-\sigma\psi)}$ has a Fourier Bessel series[6]

$$e^{iz\sin(\zeta-\sigma\psi)}=\sum_{n=-\infty}^{\infty}e^{in(\zeta-\sigma\psi)}J_n(z)$$

In this case $z=\nu\frac{p_\perp}{p_\parallel}\frac{m}{\omega}$ is a dimensionless parameter dependent on the laser strength and the perpendicular e^- response, and we have

$$e^{iS}=\sum_{n=-\infty}^{\infty}e^{i(\tilde{p}-nk)\cdot x}e^{-in\sigma\psi}J_n(z)$$

II.22

The summation index n can now be interpreted as the number of photons of energy ω that have been emitted or absorbed by the electron with a probability amplitude that is proportional to $J_n(z)$. As well the x dependence is amenable to integration when the transition amplitude is calculated later.

The dependence of ψ_{VOL} on the factor $1+\frac{e\not{k}\not{A}}{2p\cdot k}$ can be removed to an exponent as follows

Let

$$\gamma^i=-\phi_i$$

then

$$1+\frac{e\not{k}\not{A}}{2p\cdot k}=1+\frac{ea}{2p\cdot k}\not{k}(\phi_1\cos\zeta+\phi_2\sigma\sin\zeta)$$

$$=1+\frac{ea}{4p\cdot k}\not{k}[(\phi_1+i\sigma\phi_2)e^{i\zeta}+(\phi_1+i\sigma\phi_2)e^{-i\zeta}]$$

---

[6] Duff and Naylor, ref. 9, p300

and since

$$e^{\mp i\xi}\, e^{iS} = \sum_{n=-\infty}^{\infty} J_n(z)\, e^{-i(\tilde{p} - (n \mp 1)k)\cdot x}\, e^{-in\sigma\psi}$$

$$= \sum_{n=-\infty}^{\infty} J_{n\mp 1}(z)\, e^{-i(\tilde{p} - nk)\cdot x}\, e^{-in\sigma\psi}$$

we have

$$\psi_{ps}(x) = \sum_{n=-\infty}^{\infty} e^{-i(\tilde{p} - nk)\cdot x}\, e^{-in\sigma\psi}\, V_n(p)\, U$$

$$V_n(p) = J_n(z) + \frac{ea\not{k}}{4p\cdot k}\left[(\not{\epsilon}_1 - i\sigma\not{\epsilon}_2)e^{i\sigma\psi} J_{n-1}(z) + (\not{\epsilon}_1 + i\sigma\not{\epsilon}_2)\, e^{-i\sigma\psi} J_{n+1}(z)\right]$$

II.23

This form of the Volkov solution agrees with Becker *et al* (ref. 2, equations 2,3)

A modification useful for a later argument is to define

$$\vec{Y} \equiv \frac{ea}{4p\cdot k}\left[(e_1 - i\sigma e_2)e^{i\sigma\psi} J_{n-1}(z) + (e_1 + i\sigma e_2)\, e^{-i\sigma\psi} J_{n+1}(z)\right]$$

II.24

and note that

$$\mathrm{Re}\,\vec{Y} = \frac{ea}{4p\cdot k}\begin{pmatrix}\cos\psi\\ \sin\psi\\ 0\end{pmatrix}(J_{n+1} + J_{n-1})$$

$$\mathrm{Im}\,\vec{Y} = \frac{ea\sigma}{4p\cdot k}\begin{pmatrix}-\sin\psi\\ \cos\psi\\ 0\end{pmatrix}(J_{n+1} - J_{n-1})$$

II.24 a)

also that, as 4-vectors

$$Y\cdot k = 0$$

then

$$V_n(p) = J_n(z) + \not{k}\not{A}$$

II.25

and

$$V_n'(p) \equiv \gamma^0 V_n^+ \gamma^0 \qquad \text{II.26}$$

As a check we see again that $\alpha = 0$ causes the arguments of the Bessl functions to vanish. Because of A.6 and 7, only $J_0(0) = 0$, and the plane waves are found again.

III. INDUCED BETA DECAY

3.1 Beta Decay Hamiltonian

The Lagrangian formulation of classical field mechanics requires that the coordinates $\psi(x)$ and momentum $\pi(x)$ be real or complex valued fields defined on the four parameter space known as space-time. The mathematics that developed on this subject was first applied to wave phenomena, the propagation of disturbances in elastic media. Later it was found to play an important role in some dramatic achievements of this century, the theories of relativity and quantum mechanics. In special relativity the finite velocity for the propagation of signals suggests that forces operate locally as contact phenomena between the neighboring points of space; the field formalism for forces embodies this concept. In quantum mechanics a complex valued probability amplitude field $\psi(x)$ was used in a new correspondence between the objects of Mathematics and the objects of Physics to successfully account for many wave-like properties of matter. This new correlation was drawn from the objects of the Lagrangian formalism in Physics and Hilbert space in Mathematics.

Special relativity and quantum mechanics have been merged in Relativistic Quantum Mechanics and Quantum Field Theory. In the latter the wave particle dualty afforded by quantum mechanics to matter is complemented by quantizing the force field, giving it particle characteristics. For example the quanta of the Coulomb force are photons and the

quanta of the Weak force are the vector bosons. In QFT the coordinates $\psi(x)$ and momenta $\pi(x)$ are operator valued fields that satisfy canonical commutation relations (for bosons and anticommutations relations for fermions). States of a system are reprsented by rays in Hilbert space. They can be defined using the eigenvalues of complete sets of commuting observables (or "good" quantum numbers if the Hamiltonian is in this set) as indices. Convenient bases for the Hilbert space are often found in the eigenvectors of the position X, momentum P, or number N, operators. It should be remembered that Hilbert space can often be a tensor product of subspaces on which these operators are elementary.

Previous experience with quantum mechanics leads us to write a quantum field theory Hamiltonian both in terms of the coordinate fields $\phi(x)$ and $\pi(x)$, and in terms of the creation and destruction operators of quanta of the field. This technique has been useful in the oscillator and rotor problems [7]. For the simple case of a real K.G. field, the expressions are

$$\mathcal{H} = \tfrac{1}{2} \int d^3x \left(-m^2 \phi^2(x) + \nabla^2 \phi(x) + \pi^2(x) \right)$$

III.1

$$\mathcal{H} = \tfrac{1}{2} \int d^3k \; \omega \left(a_{\vec{k}}^{+} a_{\vec{k}} + a_{\vec{k}} \, a_{\vec{k}}^{\dagger} \right)$$

III.2

where $k \cdot k = m^2$ and $k_0 = \omega$. From these and the canonical

---

[7] Cohen-Tannoudji, ref. 7, sections VB,and VIA.

commutations, we can derive the Fourier transform expression

$$\Phi(x) = \frac{1}{(2\pi)^{3/2}} \int \frac{d^3k}{\sqrt{2\omega}} \left(e^{-i k\cdot x} a_k + e^{i k\cdot x} a_k^+ \right) \qquad \text{III.3}$$

These relations are often presented in a different order, but from this presentation, it should be clear that if instead of a K.G. Hamiltonian in III.1, we had started with the Dirac Hamiltonian with an e.m. interaction, as we did for the Volkov solution, then in the expression III.3 we would find the Volkov solutions in place of the D'Alembertian eigenfunctions, $e^{i k\cdot x}$, and an additional spin sum giving[8]

$$\psi(x) = \frac{1}{(2\pi)^{3/2}} \sum_{s=\pm 1/2} \int \frac{d^3k}{\sqrt{2\omega}} \left(\psi_v(\vec{k},s) \hat{a}_s(\vec{k}) + h.c. \right) \qquad \text{III.4}$$

To calculate a beta decay transition amplitude, terms leading to the governing equations for the particles involved are included in the Lagrangian. Since nuclear β decay is modelled by the decay of a nucleon within the nucleus, the particles involved are protons, neutrons and neutrinos. These are coupled to the quanta of the weak interaction, the vector bosons; as well the electrically charged particles are coupled to the external e.m. field. Both protons and electrons should couple to the external

---

[8] Formally, the Fourier transform is a distribution or functional on the vector space of "test" functions. It is a map from the vector space to the "field" named in the vector space axioms (usually the complex numbers). Here the map is between operator spaces, so these are not usual Fourier transforms, though this is what they are called.

field, but the response, or energy transfer for the proton is expected to be reduced in proportion to the mass of the particle by analogy with collisions in classical mechanics. As well the proton remains in the isolated environment of the nucleus. Therefore, as a first approximation, the term J·A is added to the Lagrangian only for the electron. This coupled current form of the interaction has been previously discussed. It is not ammenable to perturbative techniques since in the present application A is large and higher order processes may not be neglected. However, Volkov coordinate fields are the exact solutions for Dirac particles and electromagnetism. So the weak interaction terms alone may be regarded as a perturbation.

Thus we expand β decay transition amplitudes in power series for the weak coupling constant, g. For each term of a particular power, Feynman diagrams with a fixed number of weak interaction vertices can be used to picture mechanisms by which the decay is effected. In perturbative expansions the amplitude for each process is added in accordance with the principle of superposition. Each such amplitude is the product of amplitudes for the components of the Feynman diagram (in momentum representation[9]) in analogy to the

---

[9] In position representation, this product takes the form of a convolution of Green's functions for the propagation of impulses. This is noteworthy because in making an algebra out of a vector space of functionals, the convolution plays the role of vector product. (the δ functional is the identity; the Green's function is the kernel of the Green's functional which is the inverse of a differential operator.)

multiplication of conditional probabilities. The amplitude for a weak interaction boson to propagate is the "inverse" of the K.G. operator. Since the bosons have a mass of 84 GeV (ref. 6)and and the energies that concern us are only Kev, the K.G. operator and its inverse are dominated by the constant mass term

$$\frac{g}{K^2+m^2} \approx \frac{g}{m^2} \longrightarrow g$$

This constant can be absorbed into a redefined coupling constant; then the transition amplitude involves a point coupling of the fields and takes on the form of the Fermi theory of beta decay proposed in 1934 (ref. 6).

Nuclear β decay is then described by the decay of a nucleon within a nucleus. The binding energy differences between the nucleon and products along with angular momentum considerations have largely accounted for spectra variations and the wide range of β decay half lives. This success is included in the "universality" of the theory. To learn the basic techniques of β decay calculations, the decay rate for a neutron was calculated without Coulomb corrections. From published data (ref. 8) of particle masses and weak coupling constants the half life was found to be about 640 seconds;in agreement with experimental results(ref. 6, p134). The calculation and relevant weak interaction theory can be found in many sources (eg: ref. 8) and is only outlined here. First we need to develop $\mathcal{H}_\beta$ further.

Our primary interest will be in ^3H decay which is a neutron decay. To describe neutron β decay

$$n \rightarrow p^{+} + e^{-} + \bar{\nu}$$

the lowest term of the perturbation expansion is 0 and we are left with the first order term pictured as

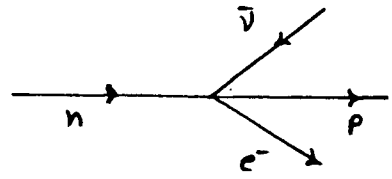

and written as

$$S = \langle n(k_n s_n) \mid \mathcal{H}_\beta \mid e^-(k_e s_e),\ p^+(k_p s_p),\ \bar{\nu}(k_\nu, s_\nu) \rangle \qquad \text{III.5}$$

where $\mathcal{H}_\beta$ is a product of the field operaters for the particles involved. As such it actually involves $\bar{\Phi}_p, \bar{\Phi}_e, \Phi_\nu, \Phi_n$ [10] for the production of the proton, electron and antineutrino and the destruction of a neutron. These are operators on a Hilbert space where the spinor and charge characters of these particles are expressed in 4 components. That $\mathcal{H}_\beta$ is hermitian ensures the unitarity of the scattering matrix S and the conservation of probability density.

General considerations will provide some information about β decay, but further detail can only be obtained from experiment. We expect that the interaction Hamiltonion that governs reference frame independent processes should be Lorentz scalars, and with our four fields written each with 4 components, there would seem to be many ways to construct these invariants. By analogy with the coupled current

[10] Another common practice is to denote the fields and the particle by the same symbol.

interaction of electromagnetism J·A, we could construct lepton and hadron probabilty density currents and couple them, or we could generalize, creating couplings of different geometrical objects and forming a linear combination.

Since after decay the remaining heavy particle is nonrelativistic, we take the nonrelativistic limit for the nucleon Dirac spinors contained in these terms. The pseudoscalar coupling vanishes; the axial vector together with the vector, and the scalar together with the tensor each reduce to

$$m_p m_n \left(C_V \chi_p^+ \sigma^0 \chi_n, C_A \chi_p^+ \sigma^i \chi_n \right) \cdot L_{V-A}$$

and

$$m_p m_n \left(C_S \chi_p^+ \sigma^0 \chi_n, C_T \chi_p^+ \sigma^i \chi_n \right) \cdot L_{S-T}$$

where $\sigma^0 = I_{2\times 2}$ and L_{V-A} and L_{S-T} are the lepton current 4-vector cofactors. In further analysis some of these factors cancel so it is convenient here to give them the shorter symbols used in the literature (eg: ref. 5)

$$M_F = \chi_p^+ \sigma^0 \chi_n$$

$$M_{GT}^i = \chi_p^+ \sigma^i \chi_n$$

and define

$$M = \left(C_V M_F, C_A \vec{M}_{GT} \right) \qquad \text{III.6}$$

The M_F and the $\vec{M}_{GT}$ terms are called Fermi and Gamow-Teller coupling respectively. The corresponding nuclear spin changes are 0 and ± 1 or 0.

For these nuclear spin changes the emitted lepton spins

must oppose or align to conserve angular momentum. That the helicities $\sigma \cdot p$ of the leptons helicities are opposed is characteristic of the V-A interaction.[11] The spin and helicity determine the emitted lepton momenta to be correlated in the aligned sense or the antialligned sense respectively for the two couplings. This is born out by β-neutrino angular correlation experiments and so the S-T terms may be discarded. The last consideration for the form of $\mathcal{H}_\beta$ is that the relativistic limit of the lepton Dirac spinors are Pauli helicity 2-spinors. The mixture of vector and axial vector parts for L_{V-A} is then

$$L \equiv L_{V-A} = \bar{U} \gamma^\mu \frac{(1-\gamma 5)}{2} V_\nu \qquad \text{III.7}$$

in order that the correct relativistic limit of the helicities be obtained. The factor $\frac{1-\gamma 5}{2}$ is now understood as the projector for right handed antineutrino chirality.

3.2 Beta Decay Rate

To find the differential β decay rate to a region of phase space, we must multiply the probability density, which is the 'square' of the probability amplitude S, by the number of states accesible, the density of phase space.

To find S^2 we first substitute expressions III.4 for the fields into III.5. We can easily evaluate the momentum integrals and spin sums because of the delta function

[11] This is shown algebraically with little difficulty.

contributions from the inner products with the creation and destruction operators. The integral over the coordinates x of the exponential factors then results in the energy momentum conservation δ function. The factors $\frac{1}{(2\pi)^{3/2}}$ are replaced by $1/\sqrt{V_B}$ in the transition to box normalization. The nucleon masses have cancelled and using III.6 and III.7 we have

$$S = \frac{g}{\sqrt{2}} \frac{(2\pi)^4}{\sqrt{4\omega_e \omega_\nu}} \frac{\delta^4(\Sigma p)}{V_B^2} M \cdot L \qquad \text{III.8}$$

Squaring we find[12]

$$(M \cdot L)^2 = tr\ M M^+ L L^+ \qquad \text{III.9}$$

MM^+ looks like a projector for which a closure-like relation might exist. Since we are looking for the unpolarized rate we sum an element of MM^+ over initial and final spins to find (no sum on μ,ν)

$$\begin{aligned}(MM^+)^{\mu\nu} &\propto \sum_{s_n} \sum_{s_p} \chi_p^+ \sigma^\mu \chi_n\ \chi_n^+ \sigma^\nu \chi_p \\ &= tr\ \sigma^\mu \sigma^\nu \\ &= 2\,\delta_{\mu\nu}\end{aligned} \qquad \text{III.10}$$

If instead of Pauli spinors we had the polarization states of a higher angular momentum basis in the above expression,

---

[12] Paraphrased: the square of an inner product is the inner product of a square, and this just reflects the commutativity of the inner product defined in the introduction.

as would arise in a more general β decay, then the summations would still give that MM^+ is diagonal and that the $(MM^+)^{\mu\mu}$ are equal for $\mu=1,2,3$. An argument from symetry would suffice for this result. An immediate consquence is that there is no interference between Fermi and Gamow-Teller terms. The spin summed MM^+ is not the identity because of the constants and the reduced matrix elements of the Wigner-Eckart theorem found along the diagonal.

Since MM^+ is diagonal we need only the diagonal elements of LL^+ in III.9 . Since we have included projectors for the antineutrino helicity we here also sum on polarizations to find Dirac projectors. Then we let the neutrino mass approach 0, a standard technique. A diagonal element of LL^+ is developed then, (no summation implied again)

$$(LL^+)^{\mu\mu} = 4 \sum_{s_e} \sum_{s_\mu} \bar{V}_\nu \frac{1-\gamma_5}{2} \gamma^\mu U_e \bar{U}_e \frac{1-\gamma_5}{2} V_\nu$$

$$= 4\, tr\, (\not{p}_\nu + m_\nu) \frac{1-\gamma_5}{2} \gamma^\mu (\not{p}_e + m_e) \gamma^\mu$$

$$= 2 \cdot tr\, \not{p}_\nu \gamma^\mu \not{p}_e \gamma^\mu$$

$$= 8 (2\, p_\nu^\mu p_e^\mu - p_\nu \cdot p_e\, G^{\mu\mu})$$

III.11

Putting this and III.10 in III.9, and the result in the square of III.8, and using $(M^i_{GT})^2 = \frac{1}{3} M^2_{GT}$ gives

$$S^2 = \frac{g^2}{2} \frac{(\delta^4(\Sigma p))^2 (2\pi)^8}{(2J_N+1)\, V_B^4} 2\left[C_V^2 M_F^2 \left(1 + \frac{\vec{p}_\nu \cdot \vec{p}_e}{\omega_\nu \omega_e}\right) + C_A^2 M_{GT}^2 \left(1 - \frac{1}{3} \frac{\vec{p}_\nu \cdot \vec{p}_e}{\omega_\nu \omega_e}\right)\right]$$

III.12

It is now convenient to replace the square of the δ function by $\delta^4(0)\,\delta^4(\Sigma P)$ and then $(2\pi)^4\,\delta^4(0)$ by the size of the 4-box $V_B T$ on which Hilbert space is defined (see appendix A). Then an integration over the undetected nuclear recoil 3 momentum is easily performed evaluating the $\delta^3(\Sigma p)$. Further simplification is achieved by integrating over the unobserved momentum of the neutrino

$$d^3p_\nu = \omega_\nu^2\, d\omega_\nu\, d\Omega$$

Then the angular integral eliminates the neutrino momentum dependence and contributes 4π. The radial integral evaluates the last δ function. Collecting these changes III.12 is now

$$S^2 = g^2 \frac{(2\pi)^5}{2J+1} \frac{2T}{V_B^4} \left[C_V^2 M_F^2 + C_A^2 M_{GT}^2 \right] \omega_\nu^2$$

III.13

where ω_o is the mass energy difference of the decaying nucleus, $\omega_\nu = \omega_o - \omega_e$, and now all masses from normalizations and field operators have cancelled. The factor in square brackets is called the nuclear part(NP).

The "marginal probability" of a decay with 4-momentum P_e, $P_e^2 = m^2$, is the product of S^2 with the density of states in the phase space. This density is finite if the coordinate space is delimited to a box. It is $V_B/(2\pi)^3$ for each of the 3 final particles and so all reference to a finite coordinate space cancels from the probability expression

$$dw' = \frac{g^2}{2J+1} \frac{2T}{(2\pi)^9} (\omega_e - \omega_o)^2 \; NP \; d^3p_e \qquad \text{III.14}$$

The decay probability per unit time is dw =dw'/T . Integrating the directions of the electron simply contributes 4π . The radial part can be written as

$$d|\vec{p}_e||p_e|^2 = \sqrt{\omega_e^2 - m^2}\; \omega_e \, d\omega_e \qquad \text{III.15}$$

giving

$$dw = \frac{g^2}{2\pi^3} \frac{NP}{2J+1} (\omega_e - \omega_o)^2 \sqrt{\omega_e^2 - m^2}\; \omega_e \, d\omega_e$$

The total decay probability is

$$w = \int_m^{\omega_o} d\omega$$

The half-life is ln2/w and when the numerical constants are inserted and the simple Fermi and Gamow-Teller neutron transition amplitudes (from III.10) are inserted, the neutron decay half life is recoverred (to about 1% accuracy).

The energies of the leptons are $\omega_e \in [m, \omega_o]$ and $\omega_\nu \in [0, \omega_o - m]$.

3.3 Induced Beta Decay Rate

The modified rate can be calculated rather easily now that the rate calculation has been set up as in the last section. Using II.23, S (III.8) is modified to

$$S = \frac{g}{\sqrt{2}} \frac{(2\pi)^4}{V_B^2} \frac{1}{\sqrt{4\omega_e \omega_\nu}} \sum_{n=-\infty}^{\infty} \delta^4(\Sigma p)\, M \cdot L_n \qquad \text{III.16}$$

where

$$L_n^\mu = e^{in\sigma\psi}\ \bar{U}_e\ V_n'\ \gamma^\mu \frac{(1-\gamma_5)}{2} U_\nu$$

III.17

and $\xi p = p_\nu + \tilde{p}_e - nk + p_p - p_n$ includes extra terms from the Volkov solution. In squaring S, eq A7 can be used to show that only the diagonal terms of the double sum on n do not vanish. As before, the nuclear spins sums determine MM^+ to be diagonal also, and the task is to evaluate

$$T_r \equiv \quad tr\ (\not{p}_e + m)\ V_n'\ \gamma^\mu \frac{(1-\gamma_5)}{2} \not{p}_\nu\ \gamma^\mu V_n$$

III.18

where μ is not summed in this expression.

Using the integral

$$\int_{Ball} d\Omega_p\ \vec{p}\cdot\vec{q} = 0 \quad \forall\ \vec{q}$$

we integrate the angular part of the neutrino momentum to find

$$T_r = 4\pi\omega_\nu\ tr\ (\not{p}_e + m)\ V_n'\ \gamma^\mu \frac{(1-\gamma_5)}{2}\ \gamma^0\gamma^\mu V_n$$

III.19

Since V_n and V_n' have even numbers of γ's, the term proportional to m vanishes. Commuting the γ^μ's towards each other gives

$$\begin{aligned}\gamma^\mu(1-\gamma^5)\ \gamma^0\gamma^\mu &= (1+\gamma^5)\ \gamma^\mu\gamma^0\gamma^\mu \\ &= (1+\gamma^5)\ (2\,G^{0\mu} - \gamma^0\gamma^\mu)\gamma^\mu \\ &= (1+\gamma^5)\ \gamma^0 \qquad \forall\mu\end{aligned}$$

Here we see that the Fermi and Gamow-Teller contributions remain in the same proportions as for the no laser case. Now we have $T_r = 4\pi\ \omega_\nu\ tr\ \not{p}_e\ V_n'\ \frac{(1+\gamma^5)}{2}\gamma^0 V_n$

or, reinserting II.23 for V_n and collecting similar terms

$$T_n = 2\pi w_\nu \left[J_n^2 \, tr \, \not{p}_e (1+\gamma^5)\gamma^0 + J_n \, tr \, \not{p}_e \left(\not{Y}^* \not{k} (1+\gamma^5)\gamma^0 + (1+\gamma^5)\gamma^0 \not{k} \not{Y} \right) + tr \, \not{p}_e \not{Y}^* \not{k} (1+\gamma^5)\gamma^0 \not{k} \not{Y} \right]$$

$$\equiv 2\pi w_\nu \, tr \left[T_1 + T_2 + T_3 \right]$$

III.20

The first term is easily evaluated using the standard trace theorems as

$$T_1 = 4 \, J_n^2 \, w_e$$

III.21

The second term is evaluated by using these theorems and the algebraic formula A6 and recalling that $Y \cdot k = Y^* \cdot k = 0$. We have

$$T_2 = -4 J_n \left(\vec{p}_e \cdot \vec{Y}^* w + w \vec{p}_e \cdot \vec{Y} + i \vec{p}_e \times \vec{k} \cdot Y - i Y^* \times p_e \cdot \vec{k} \right)$$

The triple product is cyclic. Recalling II.24 for the complex parts of Y gives

$$T_2 = -4 J_n \left[w \, \vec{p}_e \cdot (\vec{Y} + \vec{Y}^*) + i (\vec{Y} - \vec{Y}^*) \times \vec{p}_e \cdot \vec{k} \right]$$

$$= -4 J_n \, \frac{e a w}{2 k \cdot p_e} \left[(J_{n-1} + J_{n+1}) + \sigma (J_{n-1} - J_{n+1}) \right] \vec{p}_e \cdot \begin{pmatrix} \cos\varphi \\ \sin\varphi \\ 0 \end{pmatrix}$$

III.22

The third term is first modified using

$$\not{k} (1+\gamma^5) \gamma^0 \not{k} = (1-\gamma^5) \not{k} \gamma^0 \not{k} = (1-\gamma^5)(2w - \gamma^0 \not{k}) \not{k}$$

$$= (1-\gamma^5) \, 2w \not{k}$$

since $\not{k} \cdot \not{k} = 0$, to find

$$T_3 = 2\omega\, tr\, \not{p}_e \not{Y}^* (1-\gamma_5) \not{k} \not{Y}$$
$$= 8\omega(-p_e\cdot k\, Y^*\cdot Y - i\omega_e\, Y^* \times k\cdot Y - i\omega\, p_e \times Y^*\cdot Y)$$
$$= 8\omega(p_e\cdot k\, \vec{Y}^*\cdot\vec{Y} - i\,\vec{Y}\times\vec{Y}^*\cdot(\omega_e\vec{k} - \omega\vec{p}_e))$$

But $\vec{Y}\times\vec{Y}^*$ has only a third component which is multiplied by

$$(\omega_e\vec{k} - \omega\vec{p})_z = \omega_e\omega - \omega p_3 = p_e\cdot k$$

Thus

$$T_3 = 8\omega\, p_e\cdot k\,(\vec{Y}^*\cdot\vec{Y} - i(\vec{Y}\times\vec{Y}^*)_z)$$

Once again using II.24 for Y gives

$$\vec{Y}^*\cdot\vec{Y} = \frac{e^2a^2\,2}{4^2(p_e\cdot k)^2}\left(J_{n+1}^2 + J_{n-1}^2\right)$$

and

$$i(\vec{Y}^*\times\vec{Y})_z = -\frac{e^2a^2\sigma 2}{4^2(p_e\cdot k)^2}\left(J_{n+1}^2 - J_{n-1}^2\right)$$

Thus

$$T_3 = \frac{e^2a^2\omega}{p_e\cdot k}\left[\left(J_{n+1}^2 + J_{n-1}^2\right) + \sigma\left(J_{n+1}^2 - J_{n-1}^2\right)\right] \qquad \text{III.23}$$

Substituting III.21 to 21 into III.20 gives

$$T_2 = 8\omega_2\left[J_n^2\omega_e - \frac{ea\omega}{2p_e\cdot k}J_n\left(\left(J_{n-1}+J_{n+1}\right) + \sigma\left(J_{n-1}-J_{n+1}\right)\right)\vec{p}_e\cdot\begin{pmatrix}\cos\psi\\ \sin\psi\\ 0\end{pmatrix}\right.$$
$$\left. + \frac{e^2a^2\omega}{4\,p_e\cdot k}\left(\left(J_{n+1}^2 + J_{n-1}^2\right) + \sigma\left(J_{n+1}^2 - J_{n-1}^2\right)\right)\right] \qquad \text{III.24}$$

This agrees with John Hebron's Thesis (ref. 14, eq 4.3.8.)

Now recall that Ψ is the azimuthal angle of the e^- momentum. The vector $(\cos\Psi, \sin\Psi, 0)^t$ is just the direction of the component of P perpendicular to the laser flux. Thus the Ψ dependence is artificial

$$\vec{p}_e \cdot \begin{pmatrix} \cos\psi \\ \sin\psi \\ 0 \end{pmatrix} = p_\perp = \sqrt{\varepsilon^2-1}\,\sin\theta\; m$$

where θ is the polar angle. Further notational conformity and simplicity is achieved by defining energy measures as proportions of the e^- mass

$$\varepsilon = \omega_e/m \quad , \quad \varepsilon_0 = \omega_0/m$$

and $\Delta\varepsilon$

$$p_e\cdot k = \omega\omega_e - |\vec{p}|\,\omega\cos\theta = \omega m(\varepsilon - \sqrt{\varepsilon^2-1}\cos\theta) \equiv \omega m\,\Delta\varepsilon$$

and laser strength parameter

$$\nu = \frac{ea}{m}$$

It is convenient for the present purposes to average over left and right circular polarizations of the laser whereupon the σ dependent terms cancel. We have

$$T_r = 8\,\omega_\nu m\left[J_n^2\varepsilon - \frac{ea\,p_\perp}{2p\cdot k}\frac{\omega}{m}\;J_n(J_{n-1}+J_{n+1}) + \frac{\nu^2}{4\Delta\varepsilon}\left(J_{n+1}^2+J_{n-1}^2\right)\right]$$

Then using the Bessel function identity A.9 and noting that $z = \frac{ea}{p_e\cdot k}p_\perp$ (II.22) we have

$$T_r = 8\,\omega_\nu m\left[J_n^2\left(\varepsilon - n\frac{\omega}{m}\right) + \frac{\nu^2}{4\Delta\varepsilon}\left(J_{n+1}^2 + J_{n-1}^2\right)\right] \qquad \text{III.25}$$

As in the last section the integral over the recoil momentum evaluates $\delta^3(\xi\, p)$ in S^2 from III.14. And the integral over the neutrino momentum's radial component evaluates $\delta(\xi\omega)$. The factor $g^2/8\pi^4$ arises from normalizations, the coupling constant, and the neutrino angular integral as it did in III.14. We have

$$dw = \frac{g^2}{8\pi^4} \sum_{n=-\infty}^{\infty} \frac{\sqrt{\varepsilon^2-1}}{2J+1} (NP)\, m^5\, \theta(\omega_\nu)\, \omega_\nu^2 \cdot$$
$$\left[J_n^2 \left(\varepsilon - n\frac{\omega}{m}\right) + \frac{\nu^2}{4\Delta\varepsilon}\left(J_{n+1}^2 + J_{n-1}^2\right)\right] d\varepsilon\, d\Omega \qquad \text{III.26}$$

where

$$\omega_\nu = \omega_0 - \omega_e - \frac{\nu^2 m}{2\Delta\varepsilon} + n\omega \quad , \quad J_m \equiv J_m(z) \qquad \text{III.27}$$

and the θ function gaurantees that $\omega_\nu > 0$, a physical condition.

IV. NUMERICAL DECAY RATE

4.1 Summary

A computation was performed for the case of ^3H decay with the laser characteristics that have already been used in chapter 2, namely $\omega = 2eV$ and $\nu = 1$. The ratio of decay rates with and without the laser was 1.00+.01 . The error was introduced mainly by the use of asymptotic formulae for Bessel functions. Other approximations used to shorten the computation were devised to not contribute significantly to the error.

The computation was accomplished on the U.B.C. computing center's Amdahl computer (MTS operating system) using UBC's current version of Fortran. The Disspla graphics package supported at the center was used to picture various stages of the calculation, namely the Bessel functions of large argument and order, the summand of expression IV.10 and the differential decay rate.

The program that calculates the differential decay rate and the total decay rate was then used to explore other laser parameters. The results are displayed in table II. Some trends were noticed that could be verified by hand calculations. For example it was noticed that the both the decay rate and the differential decay rate did not depend on the laser frequency and this was subsequently verified analytically from the formula IV.10 . It was also noticed that the number of photons absorbed, the range of n , was

independent of ν and ω and this was also verified directly. As well the ratio of decay rates with and without the laser was seen to be independent of the laser characteristics, consistent with the proposition of no enhancement. The range of the neutrino energy was shown to be unaffected computationally and algebraically. The differential decay rate was seen to be a smooth featureless function of its parameters.

Finally the enhancement factor for beta deays other than ^3H, characterized by other decay energies ω_0 was seen to be unaffected as summarized in table II.

4.2 Kinematic Domain

The differential decay rate for an unpolarized laser, obtained by averaging left and right circular polarization expressions from III.26, is

$$dw = \frac{g^2 m^5}{8\pi^4}\, d\varepsilon\, d\Omega \sum_{n=-\infty}^{\infty} \theta(\omega_\nu)\sqrt{\varepsilon^2-1}\ \omega_\nu^2 \left[(\varepsilon - n\tfrac{\omega}{m})J_n^2 + \tfrac{\nu}{4\Delta\varepsilon}\left(J_{n+1}^2 + J_{n-1}^2\right)\right] \qquad \text{IV.1}$$

where

$$\Delta\varepsilon = \varepsilon - \sqrt{\varepsilon^2-1}\cos\theta$$

$$J_n = J_n(z)$$

$$z = \frac{ea\,p_\perp}{p\cdot k} = \nu\,\frac{m}{\omega}\,\frac{\sqrt{\varepsilon^2-1}\,\sin\theta}{\Delta\varepsilon}$$

$$\omega_\nu = m\left(\varepsilon_0 - \varepsilon - \frac{\nu^2}{2\Delta\varepsilon} + n\tfrac{\omega}{m}\right)$$

ε_0 as before is the energy available to the decay products from the nuclear process. It is the difference of nuclear

energies, so that for ^3H (as for the no laser case), $\varepsilon_0 = 1.0364$.

Inspection of z shows that it is a very large number due to the ratio $\frac{m}{\omega}$, representing approximately the number of photons absorbed. This shows that asymtotic formulae for the Bessel functions will be needed. From these formulae it can be seen that the Bessel functions vanish very rapidly for $n>z$, which establishes an upper limit of $n=z$ for the summation in IV.1 . Above this limit there is neglible contribution to the sum; an error estimate will be presented below. Also the Heaviside function, guaranteeing that the neutrino energy is positive, establishes a minimum for the summation

$$n > n_{min} = \frac{m}{\omega}\left(\varepsilon - \varepsilon_0 + \frac{\nu^2}{2\Delta\varepsilon}\right) \qquad \text{IV.2}$$

Thus n_{min} is also a large number.

For each entire summation to be nonneglible we also require n_{min} to be less than z , giving constraints on the kinematic domains in $\cos\theta$ and ε that we need to consider. We have from this condition

$$\frac{-2\varepsilon(\varepsilon_0-\varepsilon)+\nu^2}{2\sqrt{\varepsilon^2-1}} + (\varepsilon_0-\varepsilon)\cos\theta < \nu\sin\theta$$

Now set

$$A = \frac{-2\varepsilon(\varepsilon_0-\varepsilon)+\nu^2}{2\sqrt{\varepsilon^2-1}}$$

Since $n_{min} > 0$, both sides of the inequality are positive and we may square both sides to find

$$A^2 - \nu^2 + 2A(\varepsilon_0 - \varepsilon)\cos\theta + ((\varepsilon_0 - \varepsilon)^2 + \nu^2)\cos^2\theta < 0$$

IV.3

Since the quadratic expression is that of an upright parabola, the range of $\cos\theta$ is between its roots

$$\cos\theta \in [\, A(\varepsilon_0 - \varepsilon) \pm \nu\sqrt{(\varepsilon_0 - \varepsilon)^2 + \nu^2 - A^2}\,] / ((\varepsilon_0 - \varepsilon)^2 + \nu^2)$$

For these roots to be real the discriminant must be greater than 0. After some algebraic cancellations we have for the discriminant

$$-\varepsilon^2 + \varepsilon\varepsilon_0(2 + \nu^2) - (\varepsilon_0^2 + \nu^2 + \frac{\nu^4}{4}) \geq 0$$

IV.4

and ε lies between the roots of this inverted parabola

$$\varepsilon \in [\, \varepsilon_0(1 + \nu^2/2) \pm \nu\sqrt{(\tfrac{\nu^2}{4} + 1)(\varepsilon_0^2 - 1)}\,] \qquad \text{IV.5}$$

Plots of these domains for various values of ν are in fig. 3. From these plots some of the effects of the laser are already evident. For low laser intensities given by low ν the available energies for the electron are still low and the decay is still almost isotropic. But for larger laser intensities the β decay becomes more probable in the forward direction and the energy increases in magnitude and extent. The higher energy electrons are more closely aligned with the direction of the laser flux.

The neutrino energy domain can also be found. Substituting n<z in III.25 for ε_ν gives

$$\varepsilon_\nu \leq \varepsilon_o - \varepsilon - \frac{\nu^2}{2\Delta\varepsilon} + \nu\sqrt{\varepsilon^2-1}\,\sin\theta$$

Since the Bessel functions are maximized for $z \approx n$ this upper limit also represents the most probable ε_ν. From the analysis outlined in appendix C we find

$$0 < \varepsilon_\nu < \varepsilon_o - 1$$

as in unmodified decay.

To show conclusively that there is no enhancement we will have to integrate the differential rate. The first step in accomplishing this is to evaluate the sum in expression IV.1 . As already noticed n_{min} and z are both very large; the required asymptotic expressions for the Bessel functions are now presented.

4.3 Asymptotic Formulae For Bessel Functions

Four different formulae, each with varying numbers of terms have been used to approximate the Bessel functions needed here. They are derived in Watson (ref. 22) and reproduced here with the following conventions

$$\Phi = n(\tan\beta - \beta) - \pi/4$$

$$\tan\beta = \sqrt{(z/n)^2 - 1}$$

$$\tanh\alpha = \sqrt{1 - (z/n)^2}$$

They are[13] for $z > n$

$$JLT \equiv J_n(z) \sim \sqrt{\frac{2}{\tan\beta\, n\pi}}\left[\cos\Phi + \sin\Phi\left(\tfrac{1}{8} - \tfrac{5}{24}\cot^2\beta\right)/n\tan\beta + \ldots\right]$$

IV.6

[13] n is used here in place of the usual ν because of the discrete sum involved.

for $z \approx n$

$$JEQ \equiv J_n(z) \sim \frac{1}{3\pi}\left[\sin\frac{\pi}{3}\,\Gamma\left(\frac{1}{3}\right)\left(\frac{6}{z}\right)^{1/3} + (z-n)\sin\frac{2\pi}{3}\,\Gamma\left(\frac{2}{3}\right)\left(\frac{6}{z}\right)^{2/3}\right]$$

IV.7

for $z < n$

$$JGT \equiv J_n(z) \sim \frac{e^{n(\tanh\alpha - \alpha)}}{2\pi n \tanh\alpha}\left[1 - \left(\frac{1}{8} - \frac{5}{24}\coth^2\alpha\right)/n\tanh\alpha + \ldots\right]$$

IV.8

and for the transition region between $z > n$ and $z \approx n$

$$JTR \equiv J_n(z) \sim \frac{1}{3}\tan\beta\cos\left(\Phi + \frac{\pi}{4} - \frac{1}{3}\tan^3\beta\right)\cdot\left(J_{-1/3} + J_{1/3}\right) + \frac{1}{\sqrt{3}}\tan\beta\sin\left(\Phi + \frac{\pi}{4} - \frac{1}{3}\tan^3\beta\right)\cdot\left(J_{-1/3} - J_{1/3}\right)$$

IV.9

where $$J_{\pm 1/3} = J_{\pm 1/3}\left(\frac{n}{3}\tan^3\beta\right)$$

From these formulae it can be seen that the differences between J_{n+1}, J_n, and J_{n-1} for large n are negigible. Thus further simplification of the differential decay rate gives

$$d\omega = \frac{g^2 m^5}{8\pi^4}\, d\varepsilon\, d\Omega\, \sqrt{\varepsilon^2-1}\left(\frac{\omega}{m}\right)^3 \sum_{n=n_{min}}^{z} (n-n_{min})^2\left(n_{min} - n + \frac{m}{\omega}\varepsilon_0\right) J_n^2(z)$$

IV.10

Figure 4 is a composite computer drawn picture of a region of the summand of this expression as a quasicontinuous function of n using the four formulae

above. Series of these pictures were generated for n ranging from 4,000 to 8,000,000 and $n_{min}=z-500$ and $n_{min}=z-10000$. From these series the location of key features could be abstracted. Features such as the location of the last maximum or minimum before $n = z$ were found to move according to

$$\Delta n_f \equiv z - n_f = b\, z^{1/3}$$

where n_f is the value of n for a feature in question. For these features Δn_f was typically 20 to 200 and b needed to be accurate to three digits. This was obtained using graphical analysis. In table 1 "min_1" and "min_2" are the location of the minima indicated in fig. 4 . The other features are transition points between the different formulae in use, though they were not always critical. Fig. 4 illustrates that the formulae overlap for an extended interval of n .

Some useful bounds to notice are the ranges of some of the variables for the case $\nu=1$. This facilitates the determination of the total decay rate and its error. For $\nu=1$, $z \in [1.7\times10^5, 3.0\times10^5]$. Then $\tan\beta \in [0, .34]$. For $n \in [n_{min}, L_1]$, $\tan\beta \in [.048, .34]$.

4.4 The Summation

A better place to truncate the summation in IV.10 was seen from fig. 4 to be $z+100$ or $z+1.7\, z^{1/3}$ in general. Then the remaining interval of n sees a decline of the Bessel function faster than exponential since the expression $n(\alpha - \tanh\alpha) > 0$ rapidly changes from a slow initial growth

to nearly exponential growth itself. An upper bound for the error incurred by this truncation is calculated in more detail in appendix B.

The error incurred by restricting the $\cos\theta, \xi$ domain to that on which $n_{min} < z$ is calculated in a similar manner. The complementary condition $n_{min} \geq z$ gives the complementary regions of $\cos\theta$ and the same bounds on . From the calculation of appendix B it can be seen that the contribution to the total decay rate from these regions can also be neglected. If we had been able to do the complete sum on n and not had to look for the kinematic domain satisfying $n \leq z$, then the entire ξ domain would have been "allowed". Even so inverse exponential factors control the outlying regions and the summation could be found.

The calculation used Gaussian integration on the last two peaks with enough points that the error was limited by the accuracy of the asymptotic formulae. This region gives the largest contribution to the sum because of the square factor and must be assessed carefully because of the delicacy of the asymptotic formulae involved.

The main formula that gives the profile of the largest last peak of the summand is the transition region formula JTR, IV.9 . This formula has no more terms but the error is likely very low according to Watson.[18] The relative error is $\frac{24}{n} / J_n(z) < .01$

[18] Watson p252

This result led to an effort to achieve 1% accuracy in the final result. Another region of this peak uses the formula JLT, IV.7 . For 1% accuracy the second term becomes necessary for

$$(.125 - \tfrac{5}{24} / \tan^2\beta)/n\sin\beta = \pm.01$$

The maximum of $\tan\beta = .34$ restricts the left side's magnitude to far less than .01 . But near the minimum $\tan\beta = 0$, the second term dominates and $\cos\beta \approx 1$

$$\tan^3\beta = 21/n\cos\beta = 21/n$$

$$\therefore \quad z^2 - n^2 = 21^{2/3} n^{4/3}$$

$$\therefore \quad z - n = 21^{2/3} n^{4/3}/z+n \approx \frac{7.6 z^{4/3}}{2z} = 3.8 z^{1/3}$$

Thus a second term was necessary for the last two peaks before n=z. A third term is necessary for only a short region within the peak before JTR can be used and thus was neglected. For the JEQ formula similar arguments were used to find also that two terms sufficed over the range for its use. As can be seen from fig. 4 or 5, the match up of the different formulae was smooth.

In this way a multi-expression function was composed and supplied to the U.B.C. library Gaussian integration routine to sum the last peak. As well two terms of JGT were supplied for a Gaussian integration of the second last peak. There were small regions where 1% accuracy of the summand was not guaranteed, but these were regions on which the

the summand was relatively small.

The technique for summing the region $n_{min} < n < L_1$, where $L_1 = z - \Delta n$, was arranged to take advantage of the quasisinusoidal nature of the summand. The sum in question from eq. IV.10 is

$$I = \left(\frac{\omega}{m}\right)^3 \sum_{n=n_{min}}^{L_1} (n - n_{min})^2 \left(n_{min} - n + \frac{m}{\omega}\varepsilon_0\right) J_n^2(z) \qquad \text{IV.11}$$

From IV.6

$$J_n^2(z) \sim \frac{2}{\pi n \tan\beta} \cos^2\Phi$$

We may write the sum as an integral since the step size is relatively small, then arrange the terms in order of size

$$I = \left(\frac{\omega}{m}\right)^2 \frac{1}{\pi} \int_{n_{min}}^{L_1} (n-n_0)^2 \left((n_0 - n)\frac{\omega}{m} + \varepsilon_0\right) \frac{1+\cos 2\Phi}{n\tan\beta}\, dn$$

$$= \left(\frac{\omega}{m}\right)^2 \frac{1}{\pi} \int_{n_0}^{L_1} \left[\varepsilon_0 \frac{(n-n_0)^2}{\sqrt{z^2-n^2}} - \frac{\omega}{m}\frac{(n-n_0)^3}{\sqrt{z^2-n^2}} + \frac{(n-n_0)^2}{\sqrt{z^2-n^2}}\cos 2\Phi - \frac{\omega}{m}\frac{(n-n_0)^3}{\sqrt{z^2-n^2}}\cos 2\Phi\right] dn$$

$$\equiv \left(\frac{\omega}{m}\right)^2 \frac{1}{\pi}\left[I_1 + I_2 + I_3 + I_4\right]$$

IV.12

The first two integrals are easily performed[15] and presented as they were arranged for computation

$$I_1 = \varepsilon_0\left[\left(\frac{z^2}{2} + n_0^2\right)\left(\sin^{-1}\frac{L_1}{z} - \sin^{-1}\frac{n_0}{z}\right) + 2n_0\left(\sqrt{z^2-L_1^2} - \sqrt{z^2-n_0^2}\right) + \frac{1}{2}\left(n_0\sqrt{z^2-n_0^2} - L_1\sqrt{z^2-L_1^2}\right)\right]$$

[15] Though tracing suspected inconsistencies in the final result back to errors in pre-1973 CRC integral tables was not so easy. CRC edition 52, p A129, integral #220

$$I_2 = \frac{m}{\omega}\left[\left(\frac{2}{3}z^2 - 3n_0^2\right)\sqrt{z^2-n^2} - \frac{3}{2}n_0 n\sqrt{z^2-n^2} + \frac{1}{3}n^2\sqrt{z^2-n^2} + \frac{3}{2}\left(n_0 z^2 + n_0^3\right)\sin^{-1}\frac{n}{z}\right]_{n_0}^{4}$$

We may notice that

$$\frac{I_2}{I_1} < \frac{\omega}{m}(n-n_0)_{max} < .04$$

Including I_2 (which requires double precision arithmetic) could give no more than a 4% correction but it was included to achieve 1% accuracy.[16] These expectations were met in the numerical computation.

I_3 was evaluated by an " adaptive balancing" technique It was first noticed that $\cos 2\Phi = -\sin(2n(\tan\beta - \beta))$ and that the frequency did not change appreciably over each period, but rather slowly over larger changes in n. This was verified analytically using

$$\omega = \frac{d2n(\tan\beta - \beta)}{dn} = \frac{2z^2\sqrt{z^2-n^2}}{n^3}$$

and

$$T = 2\pi/\omega$$

Then each succesive half period was approximated by

$$(\text{amplitude})\times(\text{period}/2)\times\left(\int_{1/2\,\text{period}} \cos(\cdot)\right)$$

$$= (n-n_0)^2(z^2-n^2)\,n^3/z^2$$

Pairs of such approximations for neighboring half periods were first combined, then the small contribution left was accumulated. The period and the amplitude were continually

[16] Tracing persistent problems to the need for double precision in the evaluation of I_2 was also educational.

reassessed as steps of T were made from L_1 back to either z-3000 or n_{min} for n. From the data available durring the computation this correction was of order 1%.

The last integral I_4 was neglected.

4.5 Differential Decay Rate

The differential decay rate for a sequence of laser intensities from ν=.3 to 5, ω=2eV, is displayed in figs. 6 to 9. The relative sizes of the domains is most easily seen on the previous plot fig. 3. On these plots the axes are changed so as to achieve large size. The resolution of the calculation is indicated by the number of lines in the plot. The same trends as noticed from fig. 3 are noticed here.

A set of plots (not included) for a sequence of ω= .2,1,2,8 eV showed no differences, arousing suspicions that the photon energy didn't matter. Indeed this is easily verified. Starting with the expression IV.11 , we let $n' = \omega n$. Then $n'_{min} = \omega n_{min}$ and $z' = \omega z$ are independent of ω. In transforming the sum we divide by the new length between summation points, ω

$$I = \frac{1}{\omega}\frac{1}{m^2}\sum_{n'=n'_{min}}^{z'} (n'-n'_{min})^2 (n_{min}-n)/m + \epsilon_0) J_{\frac{n'}{\omega}}(z)$$

But for $1 \ll n' < z'$

$$J_{\frac{n'}{\omega}}(z) \sim \frac{2\omega}{\pi n' \tan\beta'} \cos^2\left(\frac{n'}{\omega}(\tan\beta'-\beta') - \pi/4\right)$$

where

$$\tan\beta' = \sqrt{\left(\frac{z\omega}{n'}\right)^2 - 1}$$

Thus

$$J^2_{\frac{n'}{\omega}}(z) \sim \omega J^2_{n'}(z')$$

Therefore the ω cancels, the n' may be relabelled, and we have

$$I = \frac{1}{m^2} \sum_{n=n'_{min}}^{z'} (n - n'_{min})^2 \left((n'_{min} - n)/m + \varepsilon_0 \right) J_n^2(z)$$

IV.13

independent of ω .

Additionally, the 1981 article by Becker et al shows a doubled peaked spectrum for $\nu = .3$ and a shoulder in the spectrum for $\nu = .5$ (ref. 2) This is reproduced here as fig. 10. For comparison a high resolution plot has been obtained from our study, also for $\nu = .3$. This is fig. 11 and 12, wherin no complications at the scale size indicated by Becker et al can be observed.

4.6 Total Decay Rate

From III.14 and 15 the total decay rate for β decay without a laser is

$$\omega_T = \int_1^{z_0} \int_0^{4\pi} \frac{g^2 m^5}{8\pi^4} \sqrt{\varepsilon^2 - 1}\, (\varepsilon_0 - \varepsilon)^2\, \varepsilon\, d\varepsilon\, d\Omega$$

$$= \frac{g^2 m^5}{2\pi^3} \left[\frac{(\varepsilon_0^2 + 4)(\varepsilon_0^2 - 1)^{3/2}}{30} - \frac{1}{4} \varepsilon_0^2 \sqrt{\varepsilon_0^2 - 1} + \frac{1}{4} \varepsilon_0 \ln \left(\varepsilon_0 + \sqrt{\varepsilon_0^2 - 1} \right) \right] \cdot NP$$

where NP stands for the nuclear matrix element factor. Using double precision arithmetic and the value of $\varepsilon_0 = \frac{\omega_0}{m} = 1.0364$ corresponding to Q=18.60KeV for ^3H decay, we find

$$\omega_T = \frac{g^2 m^5}{2\pi^3}\, 2.013 \times 10^{-6}$$

For the laser irradiation case we use the expressions IV.10 and IV.11 for the differential decay rate

$$dw = \frac{g^2 m^5}{8\pi^4} \sqrt{\varepsilon^2-1}\, I\, d\varepsilon\, d\Omega$$

Therefore the total decay rate is

$$w = \frac{g^2 m^5}{4\pi^3} \iint \sqrt{\varepsilon^2-1}\, I\, d\varepsilon\, d\theta$$

and from the computer calculation we obtained

$$w = \frac{g^2 m^5}{4\pi^3}\ 4.02 \pm .04 \times 10^{-6}$$

The ratio of rates is $R = \frac{W_{Laser}}{W_{no\ Laser}} = 1.00 \pm .01$ and there is clearly no enhancement due to the laser irradiation.

Table 3.2 contains the ratio of rates for different values of ν , ω , and ε_0 also. Without the further use of double precision, the limits of were determined above by n_{min} and z attaining 8 digits for ν =5 and 9 digits for ν =9 . The limit below was reached when n_{min} became close to 0 or negative for ν =.3 .Then the asymptotic formulae were no longer valid.

4.7 Program Notes

This section contains a brief summary of the larger organization and features of the main programs involved in this thesis.

The main program reads the ε and $\cos\theta$ resolution along with the input parameters ν , ω , and ε_0 , and the $\cos\theta$ bounds, and a format code for output from an input file. The desired resolution and the $\cos\theta$ bounds were based on the researcher's experience for any given run. If the $\cos\theta$ bounds chosen were too narrow the program encountered negative square roots in calculating the

summation limits n_{min} , and z, and 'crashed'. If they were too wide computer time (mainly in plotting) was sacraficed.

Thus a procedure evolved wherein first a coarse grained calculation with large $\cos\theta$ bounds was performed, followed by a finer grained one with narrower $\cos\theta$ bounds. This procedure was combined with a succesive inclusion of terms from IV.11 to show the rate calculation converge on the numbers presented in table 3.2

The program itself was modular, each module having been tested separately before the entire program was assembled.

The output of the program included the total cross section and the differential cross section data. This data was plotted in the perspective plots included by another program that called Disspla plotting routines (ref. 24). Because Disspla identifies the coordinates of a function value by its position in an array and Fortran does not fill overdimensioned multiparameter arrays contiguously it was important to reserve the exact dimensions for the differential rate data array. These numbers depended on the resolution desired and this was most useful as input for a calculation. Thus the trick of execution time dimensioning of arrays using system commands available through the system general library was invoked. Another option would have been to supply the data and its dimensions as parameters to a subroutine that does read into the array properly.

Figure 3 - KINEMATIC DOMAINS

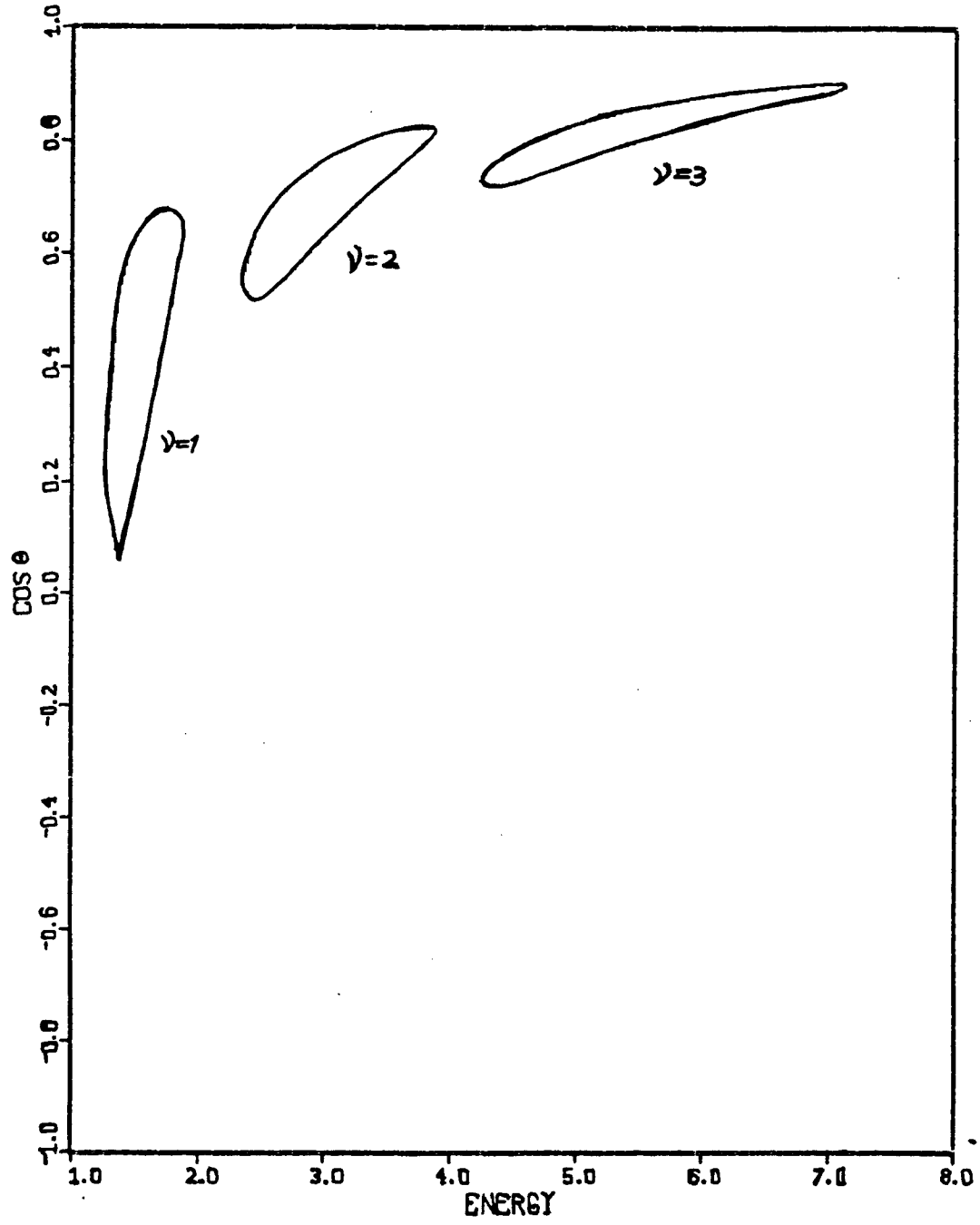

Figure 4 - SUMMAND OF IV.10

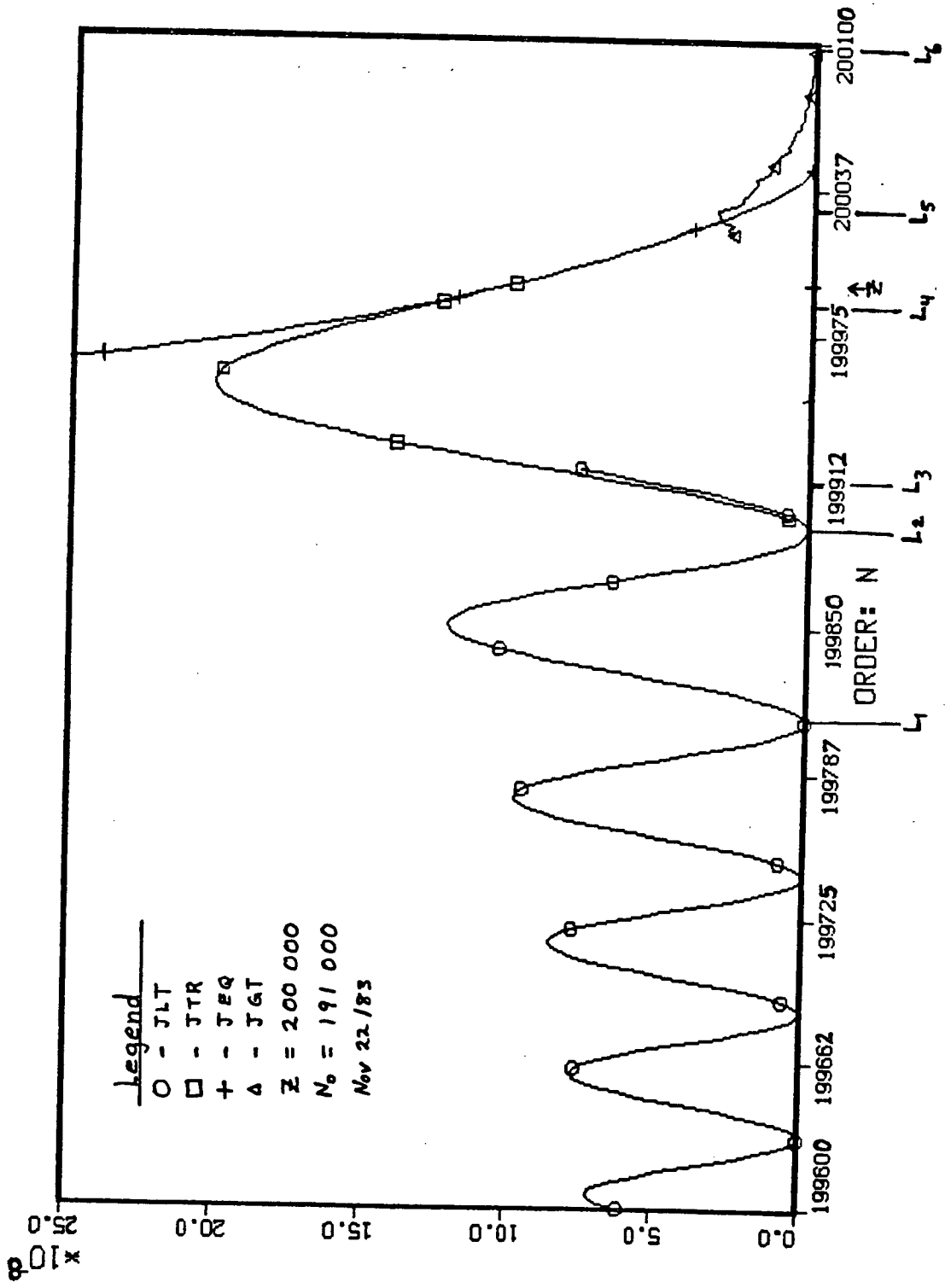

Figure 5 - OVERLAP OF ASYMPTOTIC FORMULAE

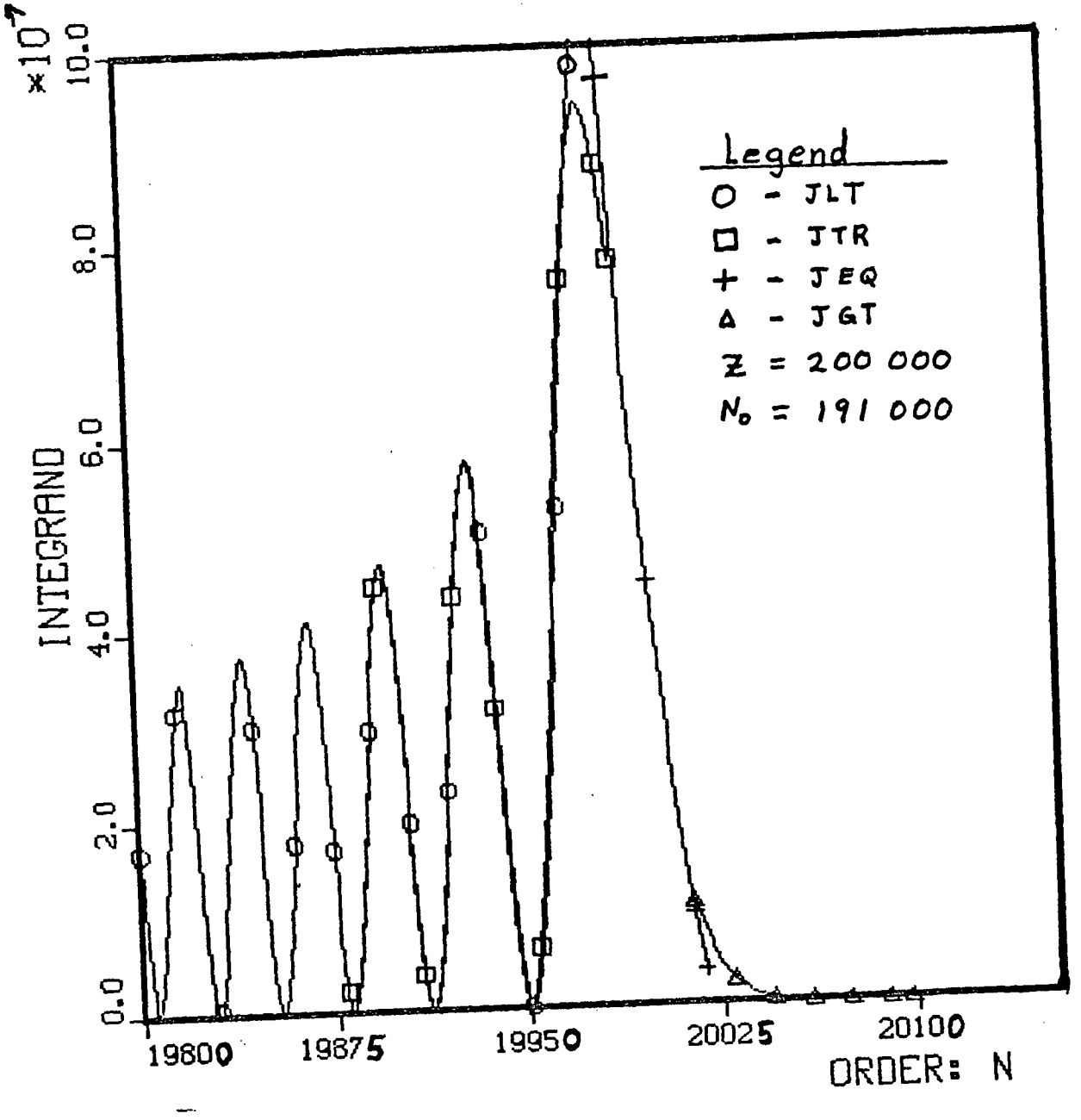

Figure 6 - DIFFERENTIAL DECAY RATE

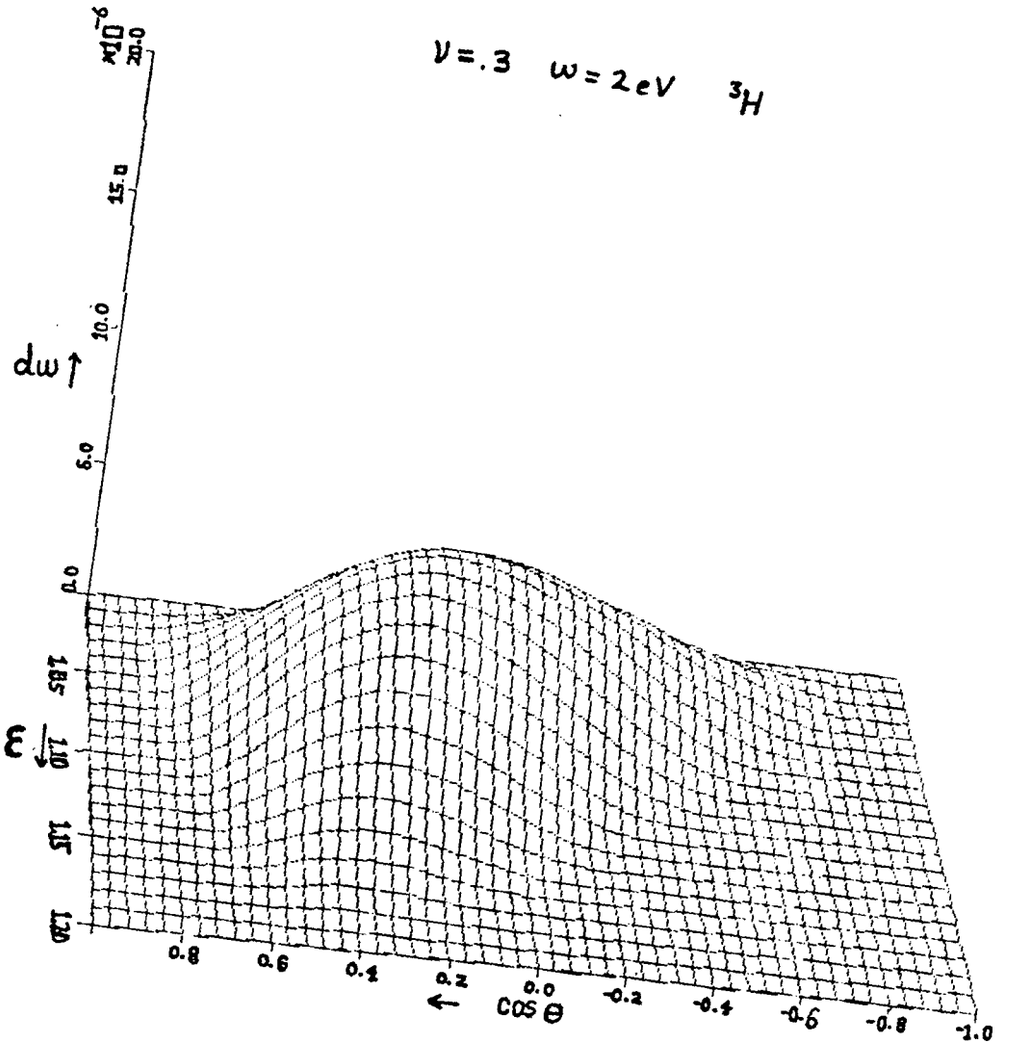

Figure 7 - DIFFERENTIAL DECAY RATE

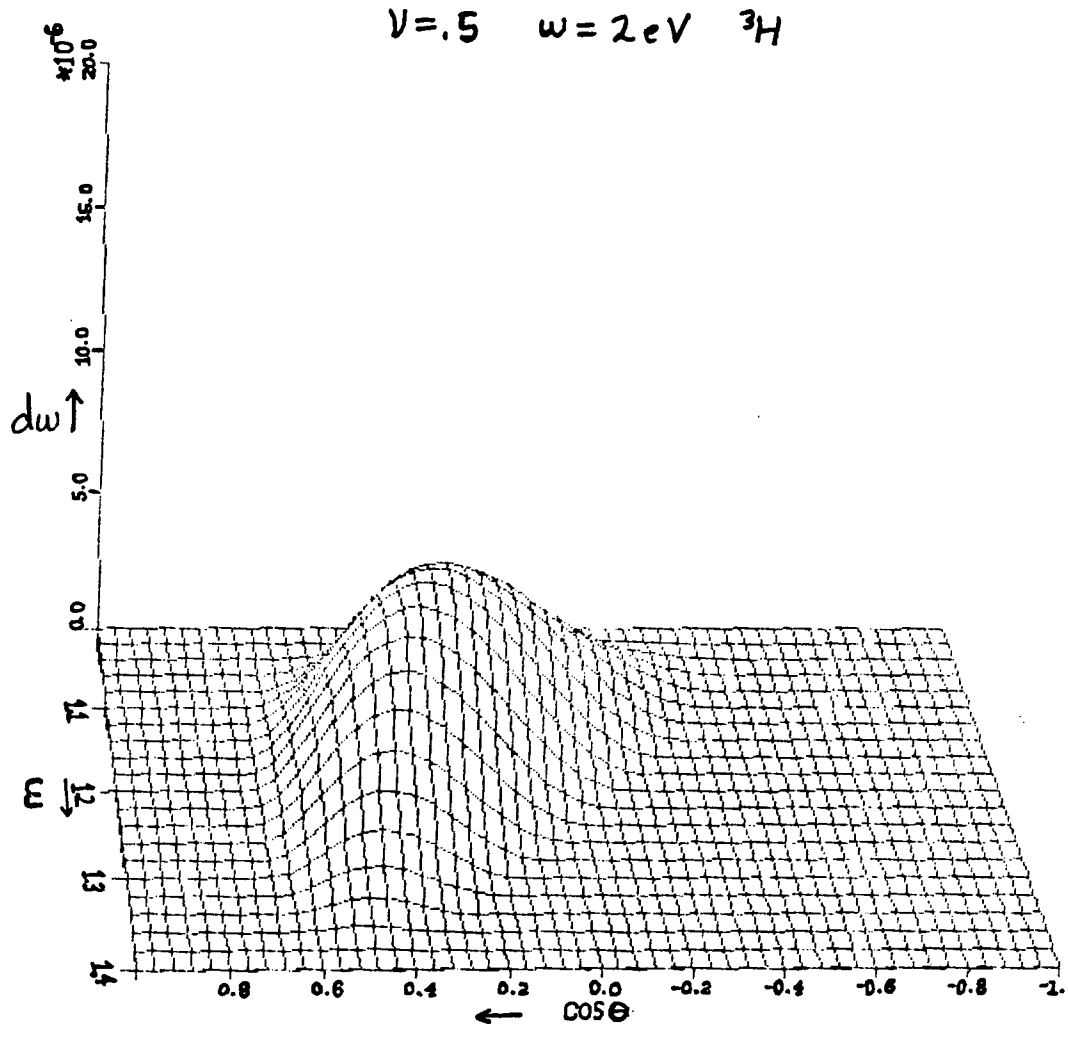

Figure 8 - DIFFERENTIAL DECAY RATE

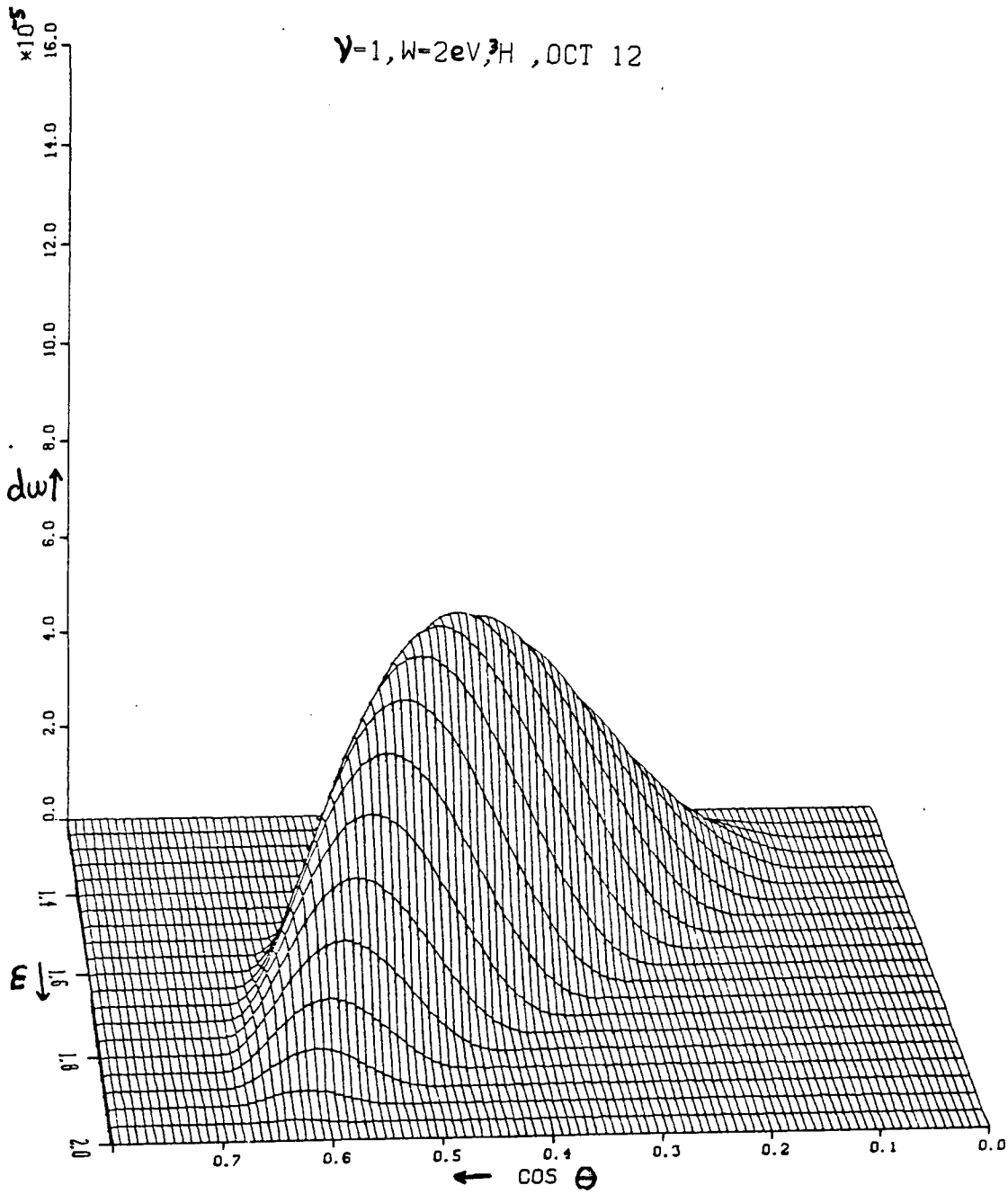

Figure 9 - DIFFERENTIAL DECAY RATE

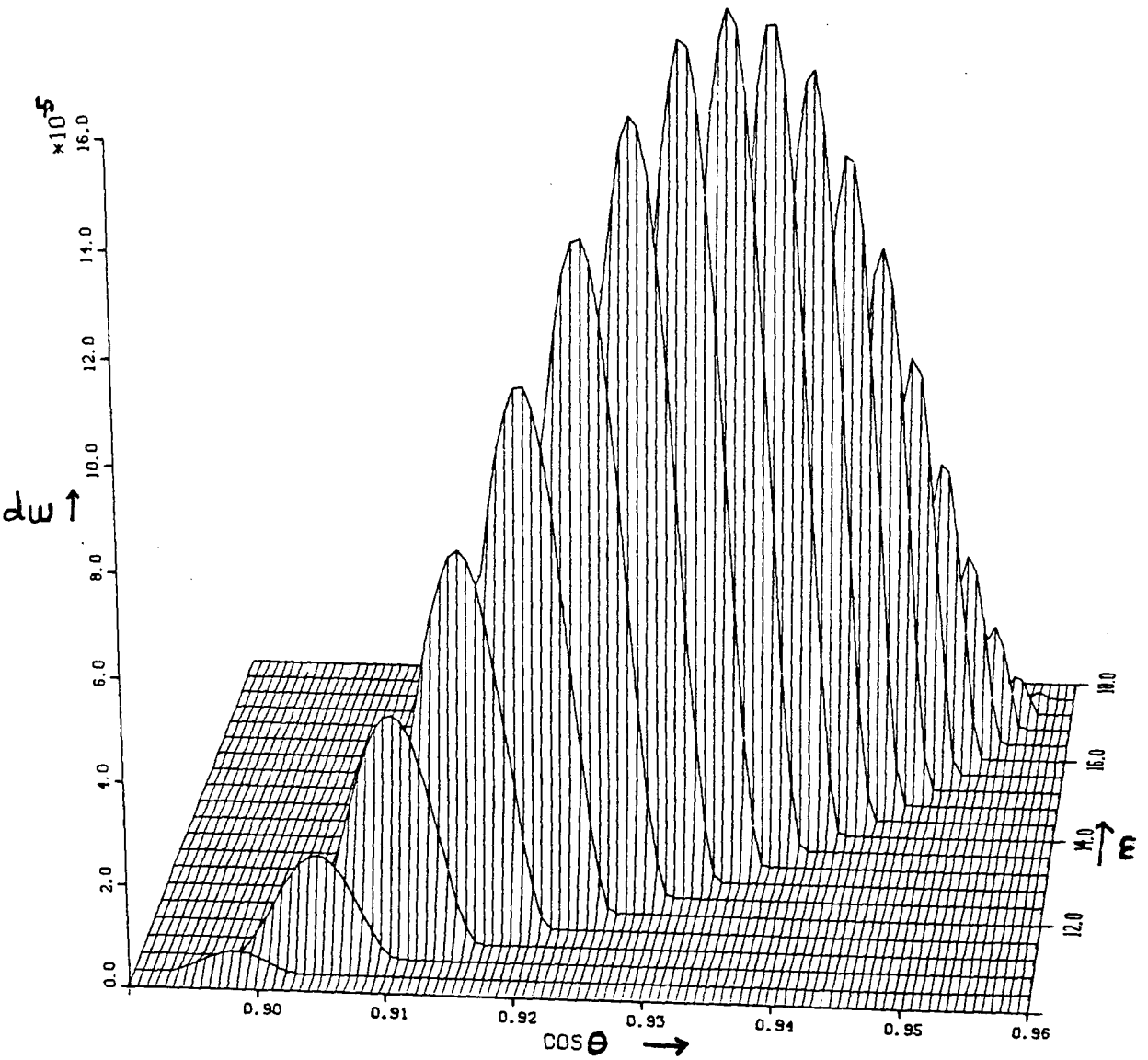

Figure 10 - ENERGY SPECTRUM OF BECKER et al

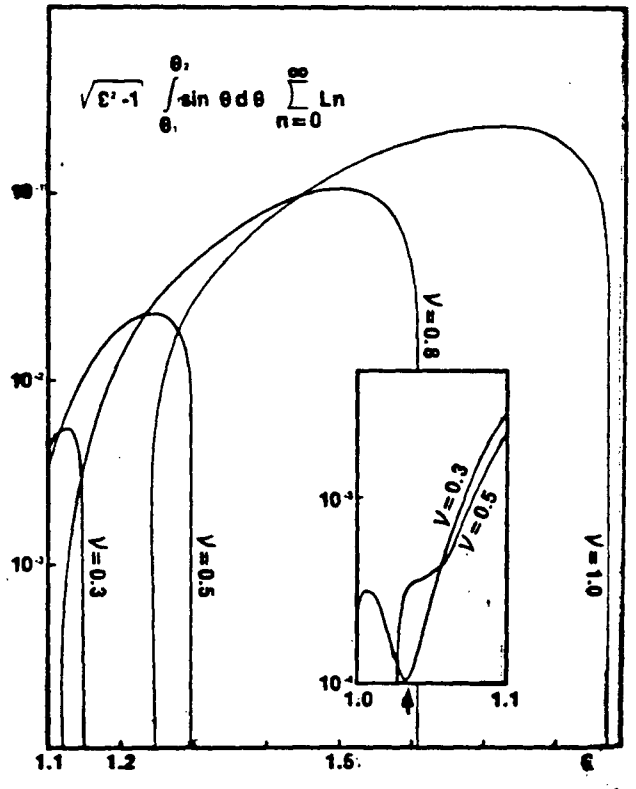

FIG. 2. Logarithmic plot of the electron spectrum of ^{3}H decay for $\nu = 0.3$, 0.5, 0.8, 1.0. The inset at the lower right shows the values for $1 \leq \epsilon \leq 1.1$ with doubled scale of the abscissa.

Figure 11 - DIFFERENTIAL DECAY RATE

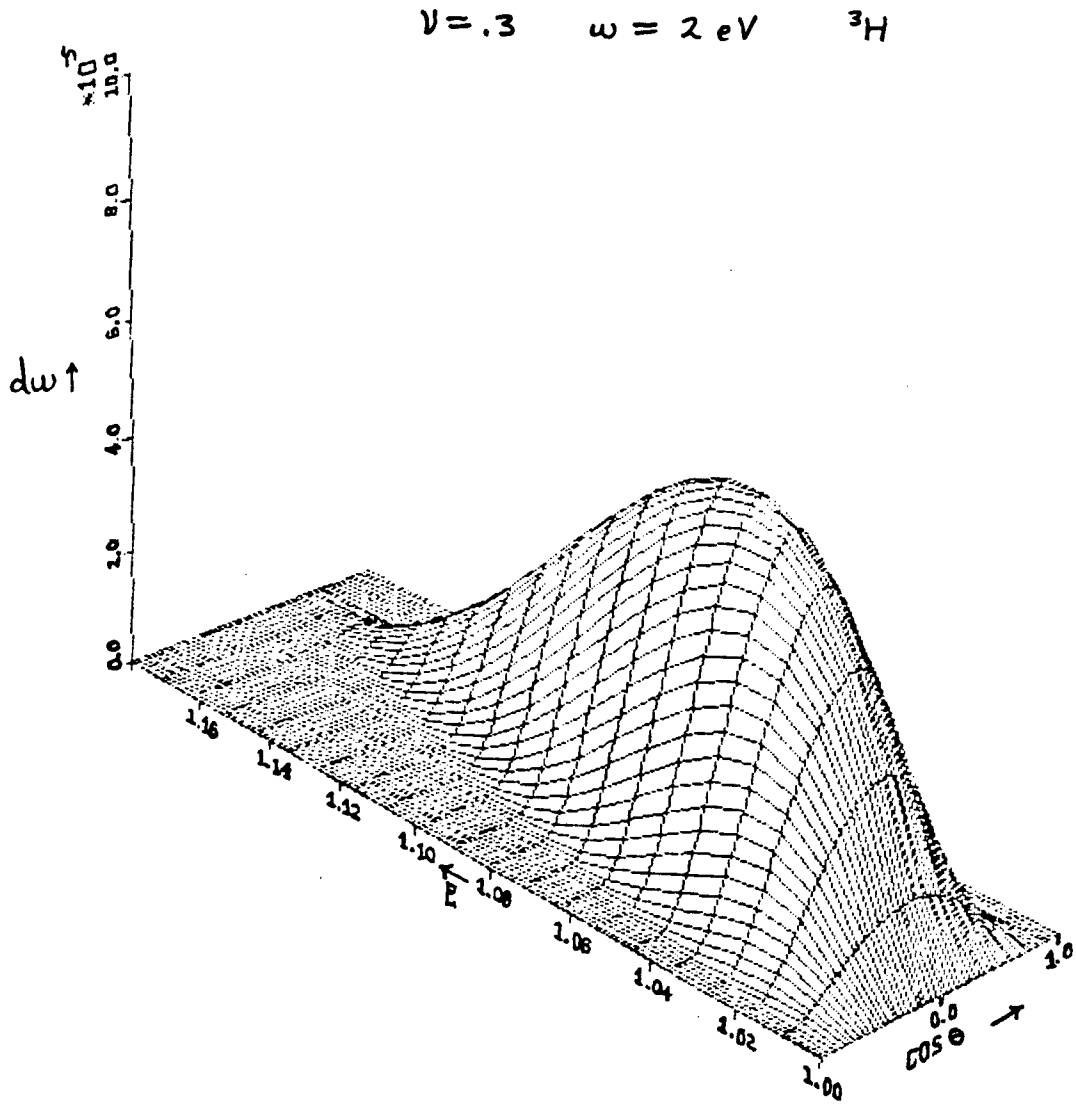

Figure 12 - DIFFERENTIAL DECAY RATE

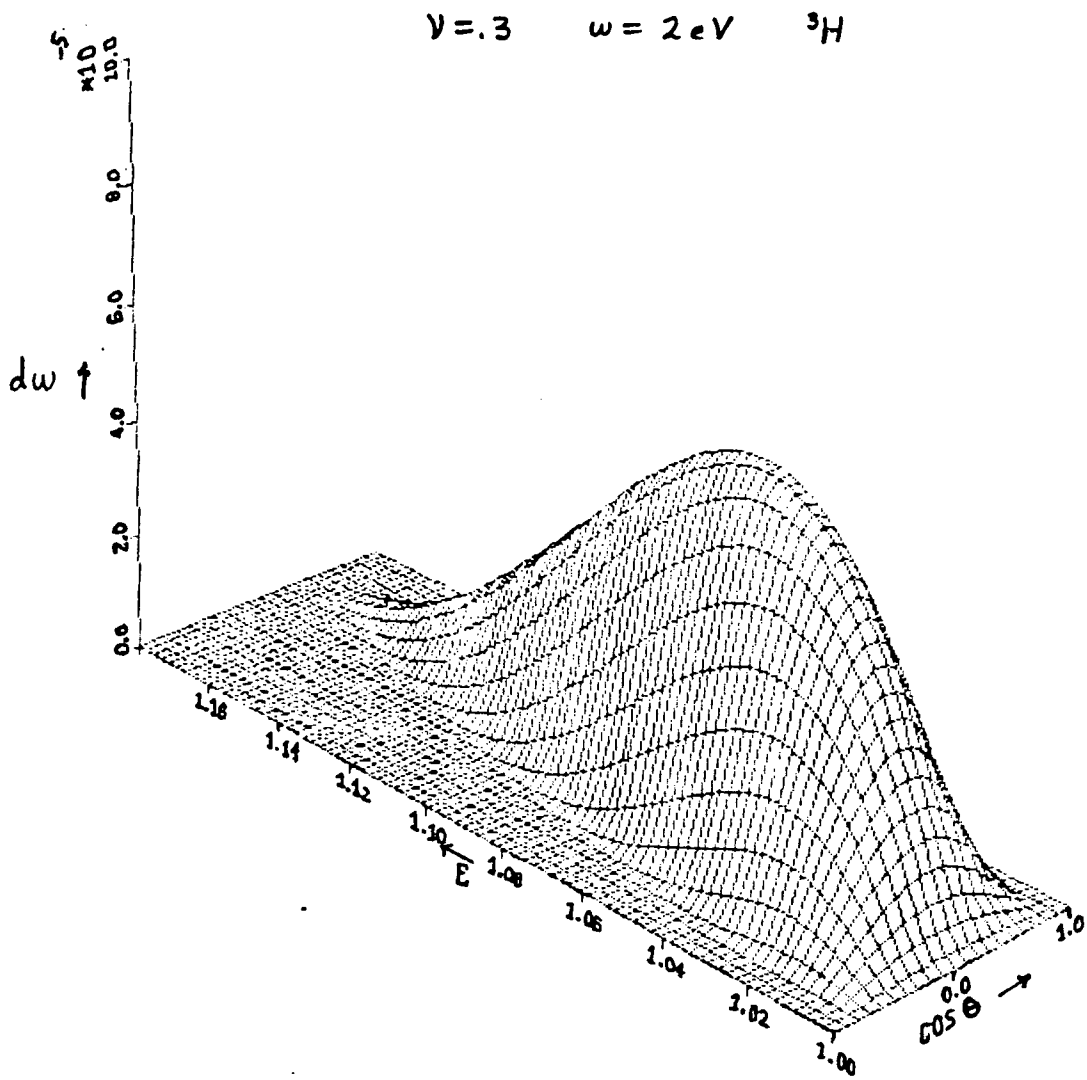

Table I - LOCATION OF FEATURES

Z →	N_0 →	$Z^{1/3}$ →	Features: min_2 Location: ΔN_2	min_1 ΔN_1	JLJ/JTK ΔN_3	JTK/JEQ ΔN_4	JEQ/JGT ΔN_5	Ratio $\frac{\Delta N_2}{Z^{1/3}}$	$\frac{\Delta N_3}{Z^{1/3}}$	$\frac{\Delta N_4}{Z^{1/3}}$	$\frac{\Delta N_5}{Z^{1/3}}$
4000	3600	15.87	30	53		2	4	1.89	3.33	.13	.25
20000	19500	27.14	51	92	38	4	10	1.88	3.38	1.4 .15	.37
	10 000		51	92	38	4	10				
200 000	194 500	58.48	108	193	88	10	25	1.85	3.30	1.5 .17	.43
	190 000		108	193	88	10	25				
2 000 000	1949 500	126.0	238	410	160	18		1.89	3.25	1.3 .14	
	1990 000		238	410	160	18					
Adopted: Value								1.86	3.31	1.4 .15	.34

Table II - NONENHANCEMENT

I (W/cm^2)	ν	ε_o	ω (eV)	$R = \frac{W_{Laser}}{W_{Laser}^{no}}$
3×10^{17}	.3	1.0364	2	1.004
4×10^{18}	1			1.005
9×10^{19}	5			1.012
2×10^{20}	7			1.000
4×10^{18}	1	1.0100	2	1.002
		1.1000		1.003
4×10^{18}	1	1.0364	8	1.006

V. CONCLUSION

The main result of this thesis is that the total decay rate for β decay is unchanged by the presence of even intense laser fields . The numerical calculations show this for a range of the laser intensity parameter $\nu \in [.3,7]$ and energies $\omega \in [2,8]$eV and a range of β decay energies $Q \in [5,50]$KeV. Furthermore the differential decay rate is found to be independent of ω and the limits of the neutrino energy spectrum are found to be unchanged (analytically and numerically) by the presence of the laser. These results were the subject of chapter 4.

In chapter 3 the differential decay rate was derived as a function of the electron energy and polar angle for β^- decay in the presence of an unpolarized intense optical laser field. The transition amplitude was derived using the Volkov electron wave function. Although the weak interaction and electromagnetic effects after creation of the electron are inseparable in these expressions the above results suggest that the laser field is not affecting the β decay process itself, but is only affecting the subsequent e^- motion. This assertion is appealing because it is consistent with the simple argument concerning the mismatch of energies (wavelengths) presented in the introduction.

Additional evidence for this assertion is the similarity (calculated) between the modification of a free electron's motion and a β decay electron's spectrum. In chapter 2 an electron initially at rest $\mathcal{E} = 1$, is found

(classically) to attain an energy, $\mathcal{E}$ =1.26 under the influence of a plane-polarized laser field with ν =1, ω =2eV. The corresponding modification of the energy range in the $^3H\,\beta^-$ spectrum (calculated quantum mechanically) is from [1,1.0364] without a laser to $\mathcal{E} \in$ [1.25,1.85] in an unpolarized laser field also with ν=1, ω =2eV. The agreement between the free e^- case and the case where the β electron has been apportioned a minimum of energy is good; however, clarification of this similarity would be achieved by an effort to compare the laser modified β^- spectrum with a calculation of the effects of a laser field on the statistical ensemble of free e^- trajectories arising from ordinary β decay.

The neutrino energy limit result, although already more persuasive of the assertion that the laser affects only the postcreation electron motion than the above e^- spectrum discussion, also might be augmented. One would examine if the detailed neutrino spectrum (not just its limits) is unchanged by the presence of the laser field.

These further studies certainly seem worthwhile for the sake of the basic physics involved. At what intensity will laser light affect nuclear process? Have they been affected at ν =1 but so as not to change β decay rates? Is the simple explanation from relative magnitudes of the energy of the laser field and the β decay the best? These are open questions.

BIBLIOGRAPHY

1. Bailin, D. "The Theory of Weak Interactions in Particle Physics" Rep. Prog. Phys. 34 pg. 491, 1971

2. Becker, W. et al. "Laser Enhancement of Nuclear Decay". Phys. Rev. Letters 47,pgs. 1262-1266, Nov. 1981.

3. Becker, W. et- al. "Becker et al. Respond:". Phys. Rev. Letters 48, pg. 653. Mar, 1982.

4. Becker,W. et al "A Note on Total Cross Sections and Decay Rates in the Presence of a Laser Field" Physics Letters 94A, pg. 131, Mar. 1983.

5. Bjorken,J.D. and Drell, S.D. Relativistic Quantum Mechanics. McGraw-Hill, New York, 1964.

6. Byrne, J. "Weak Interactions of the Neutron", Rep. Prog. Phys. 45 pg. 115, 1982

7. Cohen-Tannoudji, Diu, Laloe, Quantum Mechanics John Wiley & Sons, New York, 1977

8. deShalit, A. and Feshbach, H. Theoretical Nuclear Physics Volume1: Nuclear Structure. John Wiley & Sons, New York, 1974.

9. Duff and Naylor, Differential Equations of Applied Mathematics, John Wiley & Sons, New York, 1966

10. Enge Introduction to Nuclear Physics Addison Wesley, Toronto, 1966.

11. Feynman, R.P. The Feynman Lectures on Physics Addison Wesley, Toronto, 1965.

12. Feynman, R.P. Theory of Fumdamental Processes W.A. Benjamin, Massachusetts, 1961

13. Gersten, J.I. and Mittleman, M.H. "Comment on 'Laser Enhancements of Nuclear decay'". Phys. Rev. Letters 48, pg.651. Mar. 1982.

14. Hebron, J. "Laser Enhancement of Nuclear Beta Decay" M.Sc. Thesis, UBC, 1982.

15. Itzykson, C. and Zuber, J. Quantum Field Theory. McGraw-Hill, New York, 1980.

16. Jackson, J.D. Classical Electrodynamics 2nd Ed. John

Wiley & Sons, New York, 1975.

17. Landau, L.D. and Lifschitz, E.M. Relativistic Quantum Theory,Course of Theoretical Physics, Vol.4, part 1. Pergamon Press, Oxford, 1971.

18. Reiss,H.R. "Laser Enhancement of Nuclear Decay". Phys. Rev. Letters 48, pg. 652. Mar. 1982

19. Reiss, H.R. "Nuclear Beta decay induced by intense electromagnetic fields: Basic Theory " Phys. Rev. C27, pg. 1199 Mar. 1983

20. Ternov, I.M. et al "Change in the Beta Decay Probability due to the action of an Electromagnetic Wave." JETP letters, 37, pg. 343 Mar. 1983.

21. Volkov, "Uber eine Klasse von Losungen der Diracschen Gleichung", Z. Physik 94 pg. 250, 1935

22. Watson G.N. Bessel Functions Macmillan, Edition 2, New York, 1944

23. Standard Mathematical Tables Edition 21, The Chemical Rubber Co. Cleveland, 1973.

24. DISSPLA User's Manual, Integrated Software Systems Corp., San Diego, 1981.

APPENDIX A - NOTATION AND CONVENTIONS

Mechanics For units we set $\hbar=1=c$. For a basis of space-time we use $\hat{e}_\mu$, $\mu=\{0,1,2,3\}$. Then we have contravariant coordinates $x=(t,x)=(x^\mu)$ and the flat space covariant derivative $\partial_\mu = \partial/\partial x^\mu$. The 4-vector velocity is $u=\frac{dx}{d\tau}=(\gamma\,,\gamma\vec{v})$, but the lab frame velocity is $v=\frac{dx}{dt}(1,\vec{v})$ which is not a Lorentz vector. The metric is

$$(e_\mu\cdot e_\nu)=(G_{\mu\nu})=(G^{\mu\nu})=\begin{pmatrix}1&&&\\&-1&&\\&&-1&\\&&&-1\end{pmatrix}$$

The inner product, tr(X,Y*), for scalars is xy*, for vectors is $x\cdot y^*=x^0y^{0*}-xy^*$, and for matrices is $X_{\mu\nu}Y^{\mu\nu *}$.

Electromagnetism The electric field $\vec{E}=\vec{E}(x)$ and the magnetic field $\vec{B}=\vec{B}(x)$ can be arranged into an array

$$(F^{\mu\nu})=\begin{pmatrix}0&-E_x&-E_y&-E_z\\E_x&0&-B_z&B_y\\E_y&B_z&0&-B_x\\E_z&-B_y&B_x&0\end{pmatrix}$$

known as the e.m. field tensor because experimentally it is found to behave as a skew-symetric tensor under Lorentz transformation.

The Hodge dual is $$(F^{**})^{\mu\nu}=\tfrac{1}{2}\epsilon^{\mu\nu\alpha\beta}F_{\alpha\beta}$$

Dirac Equation The energy momentum operator in coordinate representation is

$$\hat{p}^\mu = i\partial^\mu = (i\tfrac{\partial}{\partial t}, -i\nabla)^\mu$$

For Lorentz covariance of the Dirac equation we find

$$[\gamma^\mu, \gamma^\nu]_+ = \gamma^\mu\gamma^\nu + \gamma^\nu\gamma^\mu = 2G^{\mu\nu} \qquad \text{A.1}$$

Define σ as

$$\frac{i}{2}[\gamma^\mu, \gamma^\nu]_- = \gamma^\mu\gamma^\nu - \gamma^\nu\gamma^\mu = \sigma^{\mu\nu} \qquad \text{A.2}$$

In Feynman representation these are

$$\gamma^0 = \begin{pmatrix} 1 & 0 \\ 0 & -1 \end{pmatrix} \qquad \vec{\gamma} = \begin{pmatrix} 0 & \vec{\sigma} \\ -\vec{\sigma} & 0 \end{pmatrix} \qquad \gamma^5 = i\gamma^0\gamma^1\gamma^2\gamma^3$$

Define $\not{A}$ as

$$\not{A} = A^\mu \gamma_\mu$$

For a spin ½ particle

$$(\not{p} + m)\, u(p,s) = 0$$

and antiparticle

$$(\not{p} - m)\, v(p\,s) = 0$$

Define

$$\bar{U} = U^+\gamma^0$$

Some useful results are

$$\begin{aligned} \not{p}\not{n}\not{A} &= \gamma^\mu p_\mu \gamma^\nu n_\nu \gamma^\rho A_\rho \\ &= (2G^{\mu\nu} - \gamma^\nu\gamma^\mu) n_\nu p_\mu \gamma^\rho A_\rho \\ &= 2n\cdot p\,\not{A} - \gamma^\nu(2G^{\mu\rho} - \gamma^\rho\gamma^\mu) n_\nu A_\rho p_\mu \\ &= 2n\cdot p\,\not{A} - 2\not{n}\,A\cdot p + \not{n}\not{A}\not{p} \end{aligned} \qquad \text{A.3}$$

$$\begin{aligned} \not{A}\not{A} &= \gamma^\mu\gamma^\nu A^\mu A^\nu \\ &= (G^{\mu\nu} - \sigma^{\mu\nu}) A^\mu A^\nu \\ &= A^2 \end{aligned} \qquad \text{A.4}$$

$$\not{A}\not{n}\not{A} = \ldots = -A^2 \not{n}$$

A.5

$$(\epsilon_{\alpha\beta\gamma\delta} a^\alpha b^\beta c^\gamma d^\delta) = a_0\, \vec{b}\times\vec{c}\cdot\vec{d} - b_0\, \vec{a}\times\vec{c}\cdot\vec{d} + c_0\, \vec{a}\times\vec{b}\cdot d - d_0\, \vec{a}\times\vec{b}\cdot\vec{c}$$

A.6

Mathematics One useful property of the delta function is shown here. First , the set of 'test' functions, C^∞ functions that vanish outside of a finite region R of space-time, form a vector space. The distributions form the dual space. In particular the δ functional has the property

$$\delta\,[\,F(x)] = \int \delta(x)\, f(x) dx = f(0)$$

We define the identity test function I as unity on R. Then

$$I(x) = \begin{cases} 1 & x \in R \\ 0 & \text{else} \end{cases}$$

For test functions defined on space-time we are interested in

$$\delta^2[\,I(x)] = \int (\delta^4(x))^2 d^4x = \delta^4(0) = \frac{1}{(2\pi)^2}\int e^{i0\cdot x} dx = \frac{V_B T}{(2\pi)^4}$$

also

$$\int \delta^4(x)\ \delta^4(x+y)\, d^4x = \delta^4(y) = \begin{cases} \frac{V_B T}{(2\pi)^4} & y = 0 \\ 0 & \text{else} \end{cases}$$

A.7

Some useful Bessel function identities are (ref.22)

$$J_n(z) = (-1)^n J_n(z) \qquad \text{A.8}$$

$$J_{n-1} + J_{n+1} = \frac{2n}{z} J_n(z) \qquad \text{A.9}$$

APPENDIX B - ESTIMATE FOR JGT INTEGRAL

The integral is

$$\int_{1.0005\,z}^{\infty}\left[(n-n_{min})^2(n_{min}-n+\frac{m}{\omega}\varepsilon_0)\,\frac{e^{2n(\tanh\alpha-\alpha)}}{2\pi n\tanh\alpha}\left(\sum_{m=0}^{\infty}\frac{\Gamma(m+1/2)}{\Gamma(1/2)}\,\frac{A_m}{(\frac{1}{2}\tanh\alpha)^m}\right)^2\right]dn$$

where $\tanh\alpha=\sqrt{1-z^2/n^2}$, $n\in[z,\infty]$, $\tanh\alpha\in[0,1]$, $\alpha\in[0,\infty]$. Break this into two integrals

$$I+I_2 = \int_{1.0005\,z}^{1.002\,z} + \int_{1.002\,z}^{\infty}$$

A trapeziod approximation for the first gives

$$I_1 \approx 3\times10^{2}$$

For the second use the boundary value as a maximum for the exponential factor. A change of integration variable n-1.002z=x gives gamma functions and the estimate

$$I_2 \approx 1\times10^{8}$$

Therefore the error, including the $\cos\theta$ range and the ε range is

$$E_{rror} = (1)(.5)\left(\frac{\omega}{m}\right)^3(I_1+I_2) \approx 3\times10^{-9}\times\frac{g^2}{4\pi^3}\,m^5$$

or .01 %.

APPENDIX C - NEUTRINO ENERGY

Finding the maximum of the neutrino energy both facilitates understanding laser induced β decay and provides a check of the numerical work. From IV.6 the dimensionless neutrino energy ($\mathcal{E}_\nu = \omega_\nu/m_e$) has a maximum of

$$\mathcal{E}_{\nu\,max} = \mathcal{E}_0 - \mathcal{E} - \nu^2/2\Delta\mathcal{E} + z\omega/m$$

The requirement $\mathcal{E}_\nu > 0$ gave $n_{min}\frac{\omega}{m} = \mathcal{E} - \mathcal{E}_0 + \frac{\nu^2}{2\Delta\mathcal{E}}$ and so we see that

$$\mathcal{E}_{\nu\,max} = \frac{\omega}{m}(z - n_{min})$$

Thus a maximum of $\mathcal{E}_\nu$ is also a maximum of $z-n_{min}$.

The analysis is outlined as follows. For a stationary point of $\mathcal{E}_\nu$ we have

$$\frac{d\mathcal{E}_\nu}{d\cos\theta} = 0 \longrightarrow \sqrt{\mathcal{E}^2-1}\,\sin\theta - \nu/2 = \cot\theta\;\Delta\mathcal{E}$$

$$\frac{d\mathcal{E}_\nu}{d\mathcal{E}} = 0 \longrightarrow \nu = \sqrt{\mathcal{E}^2-1}\,\sin\theta$$

From these equations a quadratic in $\cos\theta$ is found for which one root is acceptable

$$\cos\theta = \frac{\mathcal{E}-1}{\sqrt{\mathcal{E}^2-1}}$$

This gives that $\Delta\mathcal{E}=1$ and $\mathcal{E} = 1 + \nu^2/2$. We have immediatly that $0 < \mathcal{E}_\nu < \mathcal{E}_0 - 1$ and $z - n_{min} < \frac{m}{\omega}(\mathcal{E}_0 - 1)$ 9300. The latter fact was noticed first from inspection of the computational differential cross section data.

The analysis of section 4.2 can be generalized to include and verify the results of appendix C for the neutrino. Starting with the domains allowed by physical considerations

$$-1 < \cos\theta < 1 \qquad \varepsilon > 1 \qquad \varepsilon_\nu > 0$$

we seek to find the smaller domains on which the differential decay rate is nonnegligable. Setting n<z from (IV.1), defining

$$A = \frac{-2\varepsilon(\varepsilon_0 - \varepsilon_\nu - \varepsilon) + \nu^2}{2\sqrt{\varepsilon^2 - 1}}$$

and squaring to find a quadratic inequality in $\cos\theta$, we find

$$\cos\theta \in \left[\frac{-A(\varepsilon_0 - \varepsilon_\nu - \varepsilon) \pm \nu\sqrt{(\varepsilon_0 - \varepsilon_\nu - \varepsilon)^2 - A^2 + \nu^2}}{(\varepsilon_0 - \varepsilon_\nu - \varepsilon)^2 + \nu^2} \right]$$

For these limits to be real the argument of the radical must be positive. The quadratic inequality in ε gives

$$\varepsilon \in \left[(\varepsilon_0 - \varepsilon_\nu)(1 + \nu^2/2) \pm \sqrt{(\nu^2/4 + 1)((\varepsilon_0 - \varepsilon_\nu)^2 - 1)} \right]$$

Again for these limits to be real we find

$$(\varepsilon_0 - \varepsilon_\nu)^2 - 1 > 0$$

which has one admissable solution

$$\varepsilon_\nu < \varepsilon_0 - 1$$